Oxygen isotope equilibrium between ultrahigh-pressure metamorphic minerals and its constraints on Sm–Nd and Rb–Sr chronometers

YONG-FEI ZHENG, ZI-FU ZHAO, SHU-GUANG LI & BING GONG

School of Earth and Space Sciences, University of Science and Technology of China, Hefei 230026, China (e-mail: yfzheng@ustc.edu.cn)

Abstract: In the Sm–Nd and Rb–Sr isotopic geochronology of metamorphic rocks, an important question is whether radiometric systems of mineral isochrons have achieved isotopic equilibrium during a given metamorphic event and preserved the equilibrium afterwards. An analogue to mineral chronometry is O isotope geothermometry. Because the rates of Sm–Nd, Sr and O diffusion in metamorphic minerals are comparable in many cases, the state of O isotope equilibrium between metamorphic minerals can provide a test for the validity of mineral Sm–Nd and Rb–Sr chronometers. In order to illustrate this applicability, O isotope geothermometry was carried out for Sm–Nd and Rb–Sr isochron minerals from ultrahigh-pressure (UHP) eclogites and gneisses at Shuanghe in the Dabie terrane of east-central China. Although the Sm–Nd isochrons give consistent Triassic ages of 213 to 238 Ma for UHP metamorphism, the Rb–Sr isochrons give Jurassic ages of 171 to 174 Ma for the same samples. O isotope geothermometry of the gneiss, eclogite and amphibolite minerals yields two sets of temperatures of 600 to 720 °C and 420 to 550 °C, respectively, corresponding to cessation of isotopic exchange by diffusion at about 225 ± 5 Ma during high pressure eclogite-facies recrystallization and at about 175 ± 5 Ma during amphibolite-facies retrogression. The preservation of Triassic Sm–Nd isochron ages, but the occurrence of Jurassic Rb–Sr isochron ages and the regular O isotope temperatures for the same samples, suggest that rates of Sr and O diffusion in such hydroxyl-bearing minerals as biotite and hornblende are faster than rates of Nd diffusion in garnet and Sr diffusion in phengite on the scale of a hand-specimen during the amphibolite-facies retrogression. While the mineral with slow diffusivity has exerted the primary control on the homogenization rate of initial isotope ratios among isochron minerals during retrograde metamorphism, the mineral with high parent/daughter ratio has exerted the principal control on the initiation of the mineral isochron clock in response to retrogression. Valid mineral isochrons can be expected to date the timing of metamorphic resetting only if the mineral with high parent/daughter ratio has a fast rate of radiogenic isotope diffusion during the metamorphic resetting.

Oxygen is one of the main constituent elements in crustal rocks, whereas Nd and Sr are trace elements in rock-forming minerals. Oxygen isotope fractionation between coexisting minerals is a function of temperature at thermodynamic equilibrium and is thus routinely applied to geothermometry (Hoefs 1997; Valley 2001). Consistency between oxygen isotope geothermometry and cation-partition geothermometry in igneous and metamorphic rocks demonstrates that oxygen isotope equilibrium has not only been attained between the rock-forming minerals, but in many cases has not been affected by diffusion-controlled retrograde isotope exchange during rock cooling. In this regard, the oxygen isotope temperatures represent the closure temperatures of oxygen diffusion in coexisting minerals immediately after rock formation. On the other hand, the closure temperatures of oxygen diffusion in coexisting minerals vary regularly due to their differences in oxygen diffusivity at the same cooling rate (Giletti 1986; Eiler *et al.* 1993). As a result, discordant closure temperatures are observed if the minerals experienced slow cooling after rock formation.

Sm–Nd and Rb–Sr isochrons of two or three minerals have been routinely applied to dating of high-pressure (HP) and ultrahigh-pressure (UHP) metamorphic rocks (e.g. Jagoutz 1988; Gebauer 1990; Thoeni & Jagoutz 1992; Li *et al.* 1999; Luais *et al.* 2001; Thoeni 2002), but interpretation of isochron ages is not always straightforward and frequently impaired by isotopic disequilibrium and/or uncertainty in closure temperature. Nd and Sr isotope disequilibrium between isochron minerals often results in geologically spurious ages and thus has to be recognized comprehensively by means of not

From: VANCE, D., MÜLLER, W., & VILLA, I. M. (eds) 2003. *Geochronology: Linking the Isotopic Record with Petrology and Textures*. Geological Society, London, Special Publications, **220**, 93–117.
0305-8719/03/$15

only radiometric systems themselves but also other isotopic systems (e.g. O) as well as geochemical and petrological features. As illustrated by Zheng *et al.* (2002) for eclogites that were formed by UHP metamorphism in the Triassic in the Sulu terrane of eastern China, there is a direct correspondence in equilibrium or disequilibrium state between the O and Sm–Nd isotopic systems of metamorphic minerals. Some omphacite–garnet pairs from the eclogites yield O isotope equilibrium fractionations at eclogite-facies conditions, and mineral Sm–Nd isochrons give meaningful Triassic ages. In contrast, some of the omphacite–garnet pairs yield O isotope disequilibrium fractionations, and mineral Sm–Nd isochrons give geologically meaningless non-Triassic ages.

With respect to the causes for radiometric and stable isotope disequilibria among high-grade metamorphic minerals, one of the following processes can be relevant: (1) inheritance of magmatic minerals during metamorphism (e.g. Mork & Mearns 1986; Thoeni & Jagoutz 1992; Schmaedicke *et al.* 1995; Zheng *et al.* 2002), for instance, incomplete metamorphic reaction from gabbro to eclogite; (2) presence of accessory mineral inclusions in other minerals (e.g. Vance & Harris 1999; Thoeni 2002), for example, apatite, rutile and zircon in garnet and omphacite; (3) isotopic zonation (e.g. Vance & Holland 1993; Brueckner *et al.* 1996; Stowell & Goldberg 1997), for instance, polyphase growth of minerals; (4) retrograde alteration like symplectitization or replacement (e.g. Thoeni & Jagoutz 1992; Li *et al.* 1993, 2000; Zheng *et al.* 2002).

The problem for radiometric dating is sometimes analogous to a situation encountered in mineral-pair geothermometers. Isotopic geothermometers rely on the fact that at some time in a rock's history an isotopic equilibrium becomes frozen in between minerals, thus preserving a temperature. The corollary to this is that information on temperature before this time is lost because the minerals have been re-equilibrating up to that point. The process of re-equilibration is likely to be mediated by diffusion. In radiometric dating, the situation is different for different parent–daughter systems, depending on the difference in their geochemical mobility. Mineral Sm–Nd chronometers may resemble the O isotope geothermometers because of the very similar behaviour of the rare earth elements (REE) as a group during metamorphic processes. However, the situation is different for mineral Rb–Sr chronometers because of the difference in Rb and Sr mobility. Rb is an alkali metal and normally bound to O in a site having a close affinity to K, whereas Sr is an alkali-earth metal and normally bound to O in a site having a close affinity to Ca. Radiogenic Sr is produced in a site different from that normally occupied by unradiogenic Sr and is thus relatively mobile. The result is that the radiogenic Sr is susceptible to transport (gain or loss) by diffusion from the site where it is produced. The K–Ar system is an extreme case where an alkali metal decays to a rare gas that is thermodynamically unstable in the site where it is produced and is easily lost from the volume where it is analysed by an isotopic measurement. It appears that different isotopic systems in different minerals have different mobilities during the same metamorphic processes.

A critical premise in evaluating the validity of either mineral Sm–Nd or Rb–Sr isochron or O isotope geothermometry is whether the isotopic systems of interest have achieved and preserved isotopic equilibrium at the time of their formation. If not, an apparent isochron is obtained which does not date a geological event, nor can the O isotope fractionation between coexisting minerals be used for geothermometry. If isotopic equilibrium is achieved and preserved, then not only is a valid isochron obtained with a meaningful age for a given geological event, but the O isotope geothermometry also provides a temperature for mineral equilibration at the time of, or subsequent to, rock formation. Therefore, the process of diffusion plays a significant role in the distribution of trace elements and isotopes within and among minerals in igneous and metamorphic rocks that were exposed to elevated temperatures for extended periods of time.

It is essential for geochronology workers to test equilibrium or disequilibrium of radiometric systems among metamorphic minerals in practice. The state of oxygen isotope equilibrium between metamorphic minerals can provide a critical test for the validity of mineral Sm–Nd and Rb–Sr chronometers. This paper deals with a couple of aspects of the recent work in which the author has been involved to accomplish a combined study of mineral radiometric dating and O isotope geothermometry for UHP metamorphic rocks from the Dabie–Sulu orogenic belt in east-central China. The oxygen isotope data are presented here for the first time and these analyses were done on the same samples that have already been the subject of a geochronological study. Before going into these examples in detail, however, some general points are made on oxygen isotope geothermometry and comparison of O, Sm–Nd and Sr diffusivity in minerals.

Oxygen isotope geothermometry

For oxygen isotope geothermometry two basic premises are essential: (1) the isotope fractionation factor between two minerals is accurately calibrated and is sufficiently sensitive to temperature; (2) coexisting minerals were isotopically equilibrated in a specific event and compositions are frozen in. Among the several factors that influence the magnitude of equilibrium isotope fractionations are temperature, chemical composition, crystal structure, and pressure.

Calibration of oxygen isotope fractionation factors

Accurate knowledge of equilibrium isotope fractionation factors between coexisting minerals is required before oxygen isotope geothermometry can be carried out. Much effort has been devoted to the calibration of fractionation factors through theoretical calculations, experimental measurements and empirical estimates (e.g. Chacko *et al.* 2001). Among the approaches for theoretical calculations, the increment method has been most successful in providing a set of internally consistent oxygen isotope fractionation factors between minerals (Zheng 1999*a*). The calculated fractionations not only show fairly good consistency with existing experimental and/or empirical calibrations, but also yield reasonable temperatures when applied to isotope geothermometry.

Figure 1A compares the theoretical calculations of oxygen isotope fractionations between calcite and anhydrous minerals with those determined by carbonate-exchange experiments at high temperatures. Table 1 lists the parameter A of high-temperature fractionation equations in the form of $10^3 \ln \alpha_{y-x} = A \times 10^6/T^2$ for common minerals in metamorphic rocks. A set of self-consistent oxygen isotope fractionation factors for metal oxide and hydroxides, wolframate, silicate and phosphate minerals has been calculated systematically by means of the modified increment method (Zheng 1991, 1992*a*, 1993*a*,*b*,*c*, 1995, 1996*a*,*b*, 1997, 1998, 1999*a*,*b*). The validity of the theoretical calibrations at both high and low temperatures has been verified by existing data derived from: (1) isotope exchange experiments under hydrothermal or anhydrous (i.e. using carbonate as the exchange medium) conditions (e.g. Zheng 1991, 1993*a*,*b*, 1997, 1999*a*; Zhang *et al.* 1994; Zheng *et al.* 1994; Rosenbaum & Mattey 1995); (2) synthesis experiments at low temperatures (e.g. the rutile–water system: Bird *et al.* 1993; the brucite–water system: Xu and Zheng 1999; aragonite–water: Zhou & Zheng 2002, 2003); (3) theoretical calculations by statistico-mechanical methods (e.g. for magnetite and garnet: Becker & Clayton

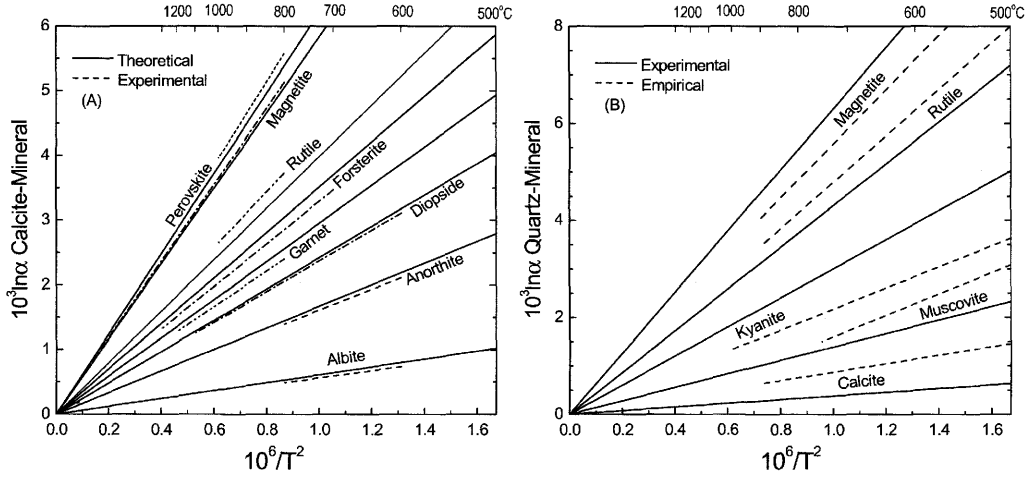

Fig. 1. A comparison of oxygen isotope fractionation factors between minerals derived from theoretical calculations, experimental determinations and empirical estimates. (**A**) Calcite–mineral systems. All theoretical data after Zheng (1999*a*). Experimental data sources: albite and anorthite (Clayton *et al.* 1989); diopside, forsterite and magnetite (Chiba *et al.* 1989); perovskite (Gautason *et al.* 1993); garnet (Rosenbaum & Mattey 1995); and rutile (Chacko *et al.* 1996). (**B**) Quartz–mineral systems. Experimental data sources: calcite (Clayton *et al.* 1989); magnetite (Chiba *et al.* 1989); muscovite and rutile (Chacko *et al.* 1996); and kyanite (Tennie *et al.* 1998). Empirical data sources: calcite (Sharp & Kirschner 1994); muscovite and magnetite (Bottinga & Javoy 1975); rutile (Agrinier 1991); and kyanite (Sharp 1995).

Table 1. *Oxygen isotope fractionation factors between metamorphic minerals at high temperatures**

Phase	Cc	Ab	Jd	Ky	Phg	An	Mus	Omp	Zs	En	Di	Hb	Bi	Zr	Gt	Tt†	Fo	Rt	Mt	Ilm
Qz	0.38	1.05	1.79	1.88	1.97	2.04	2.13	2.30	2.32	2.61	2.79	2.90	3.06	3.29	3.31	3.73	3.88	4.35	5.44	5.76
Cc		0.67	1.41	1.50	1.59	1.66	1.75	1.92	1.94	2.23	2.41	2.52	2.68	2.91	2.93	3.35	3.50	3.97	5.06	5.38
Ab			0.74	0.83	0.92	0.98	1.08	1.25	1.27	1.56	1.74	1.85	2.01	2.24	2.26	2.68	2.83	3.30	4.39	4.71
Jd				0.08	0.18	0.24	0.34	0.51	0.53	0.82	1.00	1.11	1.27	1.50	1.52	1.94	2.09	2.56	3.65	3.97
Ky					0.09	0.16	0.26	0.43	0.45	0.74	0.92	1.03	1.19	1.42	1.44	1.86	2.01	2.46	3.57	3.89
Phg						0.07	0.17	0.34	0.34	0.65	0.83	0.94	1.10	1.33	1.35	1.77	1.92	2.37	3.48	3.79
An							0.09	0.25	0.27	0.58	0.75	0.87	1.02	1.26	1.27	1.70	1.84	2.31	3.40	3.72
Mus								0.17	0.18	0.49	0.66	0.78	0.93	1.17	1.18	1.61	1.75	2.22	3.31	3.63
Omp									0.01	0.32	0.49	0.61	0.76	0.99	1.01	1.44	1.58	2.05	3.14	3.46
Zs										0.31	0.48	0.59	0.75	0.98	1.00	1.42	1.57	2.04	3.13	3.45
En											0.18	0.28	0.44	0.67	0.69	1.12	1.26	1.73	2.82	3.14
Di												0.11	0.27	0.50	0.52	0.94	1.09	1.56	2.65	2.97
Hb													0.16	0.39	0.41	0.83	0.98	1.45	2.54	2.86
Bi														0.23	0.25	0.67	0.82	1.29	2.38	2.70
Zr															0.01	0.44	0.59	1.06	2.15	2.47
Gt																0.43	0.58	1.05	2.14	2.46
Tt																	0.15	0.62	1.71	2.03
Fo																		0.47	1.55	1.88
Rt																			1.09	1.41
Mt																				0.32

Table revised after Zheng (1999*a*).

Mineral abbreviations: Ab, albite; An, anorthite; Bi, biotite; Cc, calcite; En, enstatite; Fo, forsterite; Gt, garnet; Hb, amphibole; Ilm, ilmenite; Jd, jadeite; Ky, kyanite; Mt, magnetite; Mus, muscovite; Omp, ompbacite; Phg, phengite; Qz, quartz; Rt, rutile; Tt, titanite; Zr, zircon; Zs, zoisite.

*$10^3 \ln \alpha = A \times 10^6/T^2$.

†Oxygen isotope index for titanite is recalculated to give an I-^{18}O value of 0.6846 instead of 0.7333 as previously calculated by Zheng (1993*a*).

1976; Zheng 1995; Rosenbaum & Mattey 1995) or by using Moessbauer spectroscopic data (e.g. quartz–hematite: Polyakov & Mineev 2000); and (4) empirical estimates on the basis of natural data (e.g. apatites: Zheng 1996*a*). These successes are encouraging for the application of the calculated factors to isotope geothermometry. Application of the calculated fractionations to isotopic geothermometry yields reasonable temperatures, which are consistent either with petrological temperatures for rapidly cooled rocks or with closure temperatures for oxygen diffusion in different minerals for slowly cooled rocks (e.g. Zheng *et al.* 1996, 1998, 1999, 2001, 2002; Fu *et al.* 1999; Xiao *et al.* 2000).

From the methodology of calibrating stable isotope fractionation factors it appears that theoretical calculations, experimental measurements and empirical estimates are three methods of equal importance. In some cases, the three methods can give the same results within the analytical error limit. Thus we are in a position of having some confidence in the data. In other cases, however, they do not yield the same results, so that some uncertainty arises. A number of practices have revealed that experimental measurements do not always yield correct results, nor do theoretical calculations or empirical estimates. The question is how we can justify the validity of the methods and the correctness of the results.

The development of the carbonate-exchange technique for determining oxygen isotope fractionation factors between calcite and silicate minerals has significantly enhanced the accuracy of experimental calibrations (Chiba *et al.* 1989; Clayton *et al.* 1989). However, remarkable discrepancies have been observed between such calibrations and some empirical estimates (Fig. 1B). On the one hand, the experimental fractionations of Chacko *et al.* (1996) for the calcite–muscovite and calcite–phlogopite systems are considerably smaller than the known empirical estimates. When applied to geothermometry, the experimental calibrations for these systems will yield isotopic temperatures unreasonably low in comparison with those predicted from oxygen diffusion models even under conditions of very slow cooling. It appears that the experimentally determined fractionations between calcite and micas are too small, resulting in an overestimate of the ^{18}O-enriching effect on the hydroxyl group. On the other hand, the experimental calibration of Tennie *et al.* (1998) for the calcite–kyanite system is significantly higher than the empirical estimate of Sharp (1995) and thus gives temperatures too high to be geologically reasonable. Kinetic isotope effects either in the experiments or in the nature engendered by rapid recrystallization of minerals at high-T and high-P conditions may be potential cause for the discrepancies between the experimental and empirical calibrations.

Equilibrium test for oxygen isotope geothermometry

The state of oxygen isotope equilibrium among metamorphic minerals can be simply assessed by comparing the measured fractionations with experimentally and theoretically calibrated fractionation factors at high temperatures. At thermodynamic equilibrium, the sequence of ^{18}O enrichment in the minerals is as follows: quartz > calcite > albite > jadeite > kyanite > phengite > anorthite > muscovite > omphacite > zoisite > enstatite > diopside > hornblende > biotite > zircon ≥ garnet > titanite > fosterite > rutile > magnetite > ilmenite (Table 1). If the measured fractionations between minerals follow the ^{18}O-rich sequence, with appropriate values bracketed by the high-T equilibrium estimates, oxygen isotope equilibrium is suggested between the minerals. In contrast, oxygen isotope disequilibrium is expected if the measured fractionations between mineral pairs are either too large or too small relative to the known equilibrium values even if a slowly cooling system with extreme mass balance is taken into account in evaluating the sequence of the equilibrium ^{18}O enrichment (e.g. Eiler *et al.* 1993; Jenkin *et al.* 1994).

The isothermal diagram is commonly used to present the relationship of oxygen isotope fractionations between minerals to equilibrium temperature (Javoy *et al.* 1970). It is based on the equation commonly used to relate temperature to isotope fractionation between minerals y and x over a limited range of temperature:

$$10^3 \ln \alpha_{y-x} = A_{y-x} \times \frac{10^6}{T^2} + B_{y-x}$$

where A and B are theoretically, experimentally or empirically calibrated constants, and T is the temperature in Kelvin. Rearranging:

$$10^3 \ln \alpha_{y-x} - B_{y-x} = A_{y-x} \times \frac{10^6}{T^2}$$

One mineral, normally the isotopically heaviest mineral in the rock (often quartz), is chosen as a reference mineral (*Re*). This mineral is then paired successively with every other mineral (*Mi*) in the assemblage, and values of $\Delta^{18}O_{Re-Mi} - B_{Re-Mi}$

are plotted versus A_{Re-Mi} to yield a straight line that passes through the origin if the minerals are in isotopic equilibrium by rapid cooling to give a concordant temperature. The temperature is calculated from the slope $10^6/T^2$, given that $\Delta^{18}O_{Re-Mi} = (\delta^{18}O_{Re} - \delta^{18}O_{Mi}) = 10^3 \ln \alpha_{y-x}$ at isotopic equilibrium. For oxygen isotope geothermometry of igneous and metamorphic rocks, the constant B_{Re-Mi} reduces to zero for minerals at high temperatures, $\Delta^{18}O_{Re-Mi}$ is directly calculated from measured mineral $\delta^{18}O$ values by the relation $(\delta^{18}O_{Re} - \delta^{18}O_{Mi})$, and the constant A_{Re-Mi} refers to Table 1 in practice. Then $\Delta^{18}O_{Re-Mi}$ values are plotted versus A_{Re-Mi} values in the isothermal diagram, and isothermal lines are drawn at appropriate temperatures (refer to Fig. 7).

Oxygen isotope temperatures calculated in this way are determined by: (1) the fractionation factors between different quartz–mineral pairs; and (2) the closure temperatures of the other minerals and thus oxygen diffusivity in them. The collinear extent of data points for different quartz–mineral pairs in the isothermal diagram depends on the cooling rate of the rock in question and oxygen diffusivity in the other minerals. Generally, a high temperature is obtained from a mineral that has slow rate of oxygen diffusion and a large fractionation factor when paired with quartz, whereas a low temperature is obtained from a mineral that has fast rate of oxygen diffusion and a small fractionation factor with quartz. Thus a single collinear distribution of all quartz–mineral pairs in the isothermal diagram suggests rapid cooling of the rock in question. In contrast, discordant temperatures can be yielded due either to retrograde exchange during slow cooling because of significant differences in O diffusivity among different minerals, or to isotopic resetting by a later geological event. If an assemblage has neither attained nor retained isotope equilibrium, one of the following two features occurs: (1) isotopic reversal, i.e. a negative fractionation between the reference and other minerals; or (2) unusually large fractionation that has gone much beyond the reasonable fractionation values at low temperatures by sluggish cooling. Therefore, the isotopic equilibrium relevant to O isotope geothermometry is readily testable from O isotope data themselves.

In a rock consisting of three or more minerals with different closure temperatures of oxygen diffusion, isotopic re-equilibration may continuously occur during cooling. As a result, isotope temperatures may be lower than the maximum temperature that was experienced by the rock (Giletti 1986). Thus a sequence of oxygen isotope temperatures is usually obtained for minerals with different rates of oxygen diffusion. The pair involving the refractory mineral that has the slowest diffusivity and the least affinity for ^{18}O yields the maximum temperature, whereas the pair involving the mineral that has the fastest diffusivity and the greatest affinity for ^{18}O gives the minimum temperature.

The closure temperature of element diffusion is normally defined for one mineral by assuming that it depends on diffusion in one mineral (Dodson 1973). However, it has been a common practice to pair quartz with other minerals when applying oxygen isotope geothermometry to igneous and metamorphic rocks. It appears that quartz and the other mineral do not have the same rate of oxygen diffusion and thus the same closure temperature. Therefore, a potential assumption in the quartz–mineral geothermometers is that quartz behaves isotopically as an infinite reservoir for oxygen isotope exchange with the other mineral during cooling. Although the assumption has not been proven so far, its validity is favoured by the following common consensus: (1) the common success in applying the oxygen isotope geothermometers to igneous and metamorphic rocks in nature; (2) the common occurrence of two SiO_2 polymorphs as α-quartz and β-quartz in the high-temperature rocks, which show negligible oxygen isotope fractionations between them (Zheng 1993*c*); (3) the substantial presence of SiO_2 composition in silicate rocks. In this regard, SiO_2 may behave isotopically as a pervasively active phase for oxygen diffusion within natural silicate rocks in high-temperature geological processes.

Diffusion of O, Sm–Nd and Sr in metamorphic minerals

Diffusion is the thermally activated, relative movement (flux) of atoms or molecules that occurs in response to forces such as gradients in chemical potential or temperature. Diffusion is spontaneous and, therefore, must lead to a net decrease in free energy. Mass transport by diffusion across mineral grains and along grain boundaries plays an important role in many geological processes, including isotopic exchange between minerals and between mineral and fluid, growth of minerals by metamorphic reactions, and deformation by diffusion creep and pressure solution. Kinetics of diffusion penetration in single crystals or polycrystalline aggregates change with both temperature and time, in such a way that the impact of rapid diffusion in grain boundaries on the overall scale

of mass transport is minimal, whereas slow rates of volume diffusion exert the primary control on the distance of mass transport and thus the extent of isotopic equilibrium or disequilibrium among metamorphic minerals.

Fundamental aspects

The generation of metamorphic rocks entails the motion of chemical entities, often on an atomic scale by diffusion between minerals. The rates at which metamorphic processes proceed can be dependent on the type and rate of diffusion of the chemical components in the system. Processes of hydrothermal alteration or mineral reaction are controlled, in part, by the diffusion of chemicals over the surfaces (*surface diffusion*) or along grain boundaries (*grain-boundary diffusion*), as well as through the body of mineral grains (*volume diffusion*). Rates of crystal growth can be dependent on diffusion rates in a melt.

Rates of diffusion generally increase with increasing temperature, and the relationship is expressed by the Arrhenius equation:

$$D = D_0 \exp\left(-\frac{Q}{RT}\right)$$

where D is the diffusion coefficient (units of cm^2/s), D_0 is the frequency factor which is usually a constant for a diffusing species in a particular medium, Q is the activation energy (units of kJ/mol) which gives a quantitative indication of the energy required to initiate movement of the chemical component involved in the diffusion processes, and R is the gas constant (8.3144 J/K mol). The temperature dependence on diffusion rate is normally shown on an Arrhenius plot of $\ln D$ versus reciprocal temperature (Fig. 2). Compilations of Arrhenius parameters for diffusion of elements of geological interest have been presented by Brady (1995), Zheng & Fu (1998), and Cole & Chakraborty (2001).

Closure temperature is a useful concept for comparing the relative diffusivities of different elements in the same minerals and the same elements in different minerals. Closure temperatures of radiometric systems can be estimated on the basis of existing experimental and empirical studies, assuming that loss of radiogenic isotopes during cooling was dominated by diffusion processes (Dodson 1973, 1979). It is commonly assumed that below the closure temperature isotopic exchange effectively ceases during geological processes. Although this concept has been applied to both stable and radiogenic isotopes, and to cations, its meaning may be somewhat different in different applications. For many radiogenic systems, the loss of a trace element (e.g. Sr, Pb, Ar) is complete once it reaches a grain boundary, meeting the conditions that a mineral is surrounded by an infinite, well-mixed reservoir of the element of interest. Thus, the closure temperature for a radiogenic system is the temperature at the time corresponding to a mineral's apparent age. For major elements, however, the grain boundary is not a large reservoir and a mineral can only change in composition if there is another phase with which to exchange. Hence, the properties of other minerals or fluids in a rock affect the actual closure of diffusive exchange. Furthermore, the transition to closure is not a single temperature; diffusion slows down, but does not stop at any geological temperature (Valley 2001).

While many processes can contribute to exchange, the most successful treatments of closure temperature have been in systems that are dominated by volume diffusion into a crystal from its grain boundary. The extent of isotopic exchange by volume diffusion depends on the phases present, the nature of the grain boundary, diffusion coefficients, activation energies, crystal size (or diffusion distance), and thermal history (Dodson 1973, 1979). It has been the common consensus that the faster the rate of element diffusion in minerals, the lower the closure temperature under the same conditions. Thus closure temperatures are higher for lower values of diffusion coefficients, larger grain sizes, or faster cooling. During slow cooling, the time at which the rock finally records an apparent temperature equal to the closure temperature is much later (and at lower T) than the time that the rock cooled through this temperature (Valley 2001). In fact, the closure temperature for various stable and radiogenic isotopes in minerals is dependent on a number of factors, including grain size, major element composition, the nature of coexisting phases, fluid availability, and the thermal history experienced by each individual sample. Therefore, a mineral does not possess a unique closure temperature for any given element.

Because of diffusion-controlled isotope exchange during rock cooling (e.g. Cliff 1985; Giletti 1986, 1994; Ganguly & Ruiz 1987; Jenkin *et al.* 2001), there may be a difference in timing between an isotopic age and a geological event. This is equivalent to the difference in temperature between rock formation and the diffusion closure of radiogenic isotopes in constituent minerals. If the temperature difference is very small, the time difference is also small and thus the radiometric age can serve as a close proxy for the timing of rock formation. If the temperature

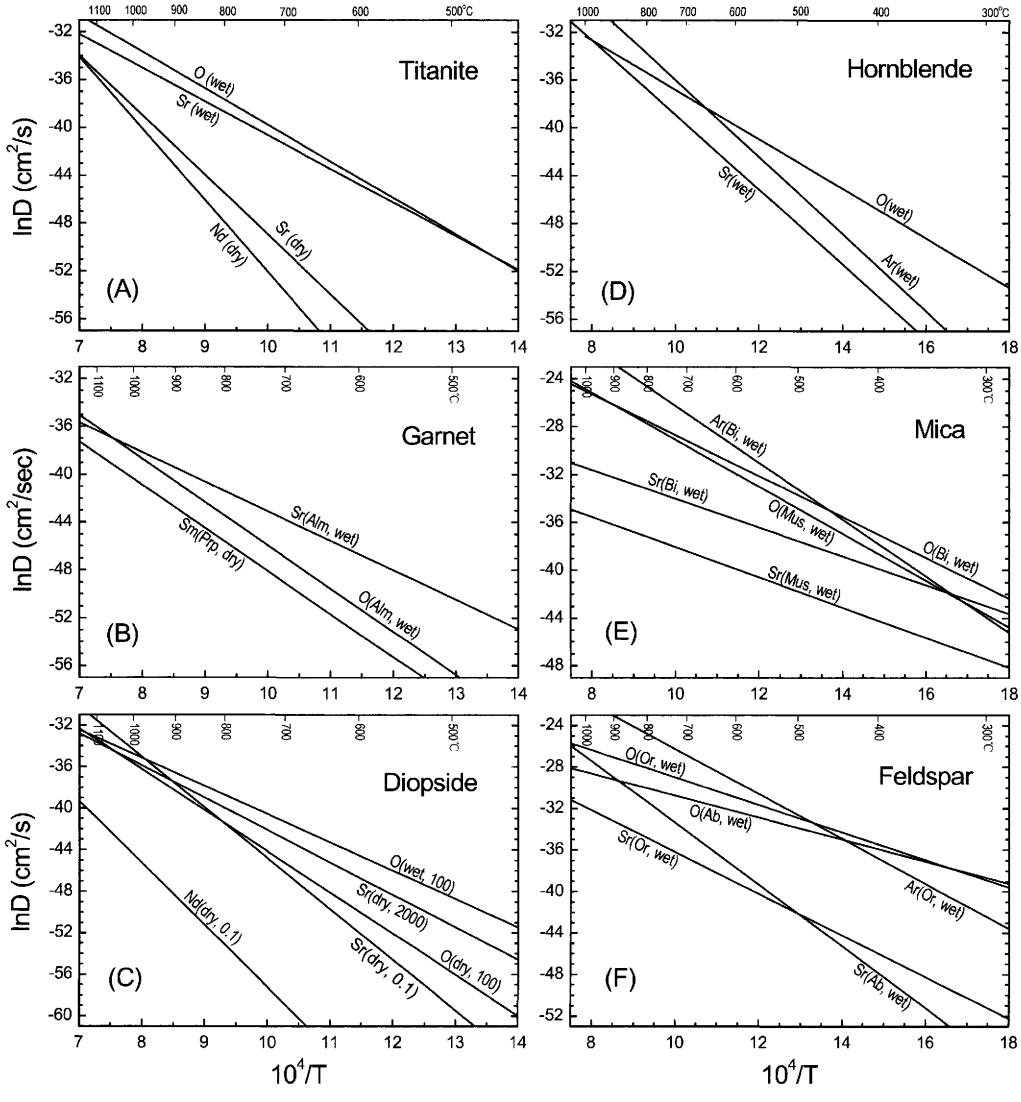

Fig. 2. Comparison of O, Sr, Sm–Nd and Ar diffusivities in mafic and felsic minerals (data and abbreviations after Table 2 with * for relevant minerals). Numbers in parentheses denote the experimental pressure (in MPa).

difference is large, or a protracted process of isothermal exhumation is involved, the isotopic age may record a time at which the retrograde isotope exchange ceased within the rock during cooling (the so-called 'cooling age').

Both concordant and discordant ages have been dated for igneous and metamorphic rocks in the past three decades by means of either different radiometric techniques (e.g. U–Pb, Sm–Nd, Rb–Sr and Ar–Ar) on the same minerals or the same technique on different minerals. The extent of concordance or discordance depends primarily on the cooling rate of the rock in question and cation diffusivity in the dated minerals. It appears that concordant ages can be obtained from the assemblages that experienced rapid cooling, whereas discordant ages are yielded due to either slow cooling or differential resetting by a later event.

Comparison of O, Sm–Nd and Sr diffusivities

Recent years have seen a considerable increase in the body of data on diffusion in minerals of petrological interest; much work has been done

on the diffusion of O, REE, Sr and other elements by means of experimental determinations and empirical estimates. Table 2 gives a compilation of typical diffusion coefficients for the stable and radiogenic isotopes dealt with in this paper, and some typical examples are illustrated in Figure 2A, B and C for mafic minerals and in Figure 2D, E and F for felsic minerals. All of the available experimental data show two general rules for cation diffusion in silicate minerals: (1) diffusion rates decrease with increasing valence, i.e. $M^{1+} > M^{2+} > M^{3+} > M^{4+}$; (2) at the same valence, the smaller the cation radius, the faster its diffusion rate. Clearly, ionic radius makes for modest differences in the diffusion kinetics, while the valence makes differences of orders of magnitude.

The first rule is consistent with the natural observation that shows a faster rate of Sr transport relative to Nd in garnet from metamorphic rocks (Vance & O'Nions 1990, 1992), but it is at odds with the observation that rate of Pb transport is much slower than rates of Nd and Sr in garnet from a granulite-facies coronite (Burton *et al.* 1995). This can be explained by connecting the mobility of radiogenic isotopes with the mobility of their parent isotopes in the same minerals. U is a tetravalent element, so that radiogenic Pb^* is produced in a site different from that normally occupied by the common Pb^{2+} and is thus relatively immobile. On the other hand, Rb is a monovalent element, so that radiogenic Sr^* is produced in a site different from that normally occupied by the common Sr^{2+} and is thus relatively mobile. As a result, the radiogenic Sr^* is very susceptible to transport (gain or loss) relative to radiogenic Pb^* by diffusion from the sites where they are produced. The situation is different for the Sm–Nd radiometric system because of the similarity in REE diffusivity. The result is that the radiogenic Nd^* behaves isotopically like the radioactive Sm^{3+} when transporting by diffusion from the site where it is produced. Consequently, diffusion rates of radiogenic Pb^*, Nd^* and Sr^* in the same minerals are basically similar to those of their parent elements: $Rb^{1+} \geq Sr^* > Sm^{3+} \geq Nd^* > Pb^* \geq U^{4+}$.

An inspection of diffusion data available for Nd, Sr and O in minerals (Fig. 2) shows that the diffusion rate of the radiogenic isotopes is slower than that of O in some minerals, but similar to or faster than O in other minerals. As a result, O isotope equilibrium between coexisting minerals can serve as a guide to evaluate whether Nd and Sr isotopic equilibrium exists under the same conditions. For example, the diffusion rates of O and Nd in garnet are similar to each other but slower than those of Sr diffusion at the same temperatures (Fig. 2B). If O isotope equilibrium involving garnet has been disturbed by later geological processes (e.g. retrograde metamorphism, hydrothermal alteration and so on), the validity of Sm–Nd and Rb–Sr mineral isochrons has to be suspect. Likewise, the diffusion rates of O and Sr in diopside are generally similar to each other but much faster than those of Nd diffusion (Fig. 2C). If O isotope equilibrium involving pyroxene has been disturbed by later processes, the validity of Rb–Sr mineral isochrons would be in doubt but the validity of Sm–Nd mineral isochron can still hold. On the other hand, the rates of O diffusion in feldspar and mica are faster than those of Sr diffusion (Fig. 2E and F), thus attainment of isotopic equilibrium in a mineral Rb–Sr system suggests achievement of O isotope equilibrium in the same minerals. In contrast, preservation of O isotope equilibrium in minerals indicates that the equilibrium mineral Rb–Sr system was not disturbed by later geological events and, therefore, that the mineral Rb–Sr isochron provides a meaningful age.

Because the same elements can exhibit different rates of diffusion in different minerals and because different elements can show similar rates of diffusion in the same mineral, both equilibrium and disequilibrium systems can occur in nature and diffusion kinetics governing isotopic exchange among minerals is generally the rate-limited step. For equilibrium systems in igneous and metamorphic rocks, rapid cooling results in preservation of isotopic equilibrium, slow cooling causes partial resetting, and protracted high-temperature processes can lead to isotopic re-equilibration and thus complete resetting. On the other hand, disequilibrium systems occur due to short-lived or low-temperature processes during partial melting, metamorphic reaction or hydrothermal alteration. A field-based study of diffusion kinetics can hence place quantitative constraints on the timescale that it takes to achieve isotopic equilibrium. This can be successfully accomplished only if the following conditions can be met: (1) diffusion rates and mineral modes are known for all the major phases; (2) both parent and daughter elements diffuse at similar rates; and (3) diffusion operated on similar length scales in the analysed phases or else on the scale of sampling (Giletti 1991).

Dabie UHP metamorphic rocks

Geological settings

Since the discovery of coesite and microdiamond inclusions in eclogites from the Dabie terrane in east-central China (e.g. Okay *et al.* 1989;

Table 2. *Arrhenius parameters for O, Sm–Nd, Sr and Ar diffusion in minerals*

Mineral*	Abbr.	Medium	Orientation	T (°C)	P (Mpa)	Q (kJ/mol)	$\ln D_0$ (cm^2/s)	Reference
O								
Quartz	Qz	Wet	//c	500–550	100	284 ± 92	5.25	Giletti & Yund (1984)
Quartz	Qz	Wet	//c	560–850	100	142 ± 4	−14.73	Giletti & Yund (1984)
Quartz	Qz	Dry	//c	745–900	0.1	159 ± 13	−17.68	Sharp *et al.* (1991)
Calcite	Cc	Wet	isotropic	400–800	100	173 ± 6	−9.57	Farver (1994)
Calcite	Cc	Dry	//c	600–800	100	242 ± 39	−4.89	Labotka *et al.* (2000)
Aragonite	Arg	Wet		300–1200	100	208	−10.78	Zheng & Fu (1998)
Aragonite	Arg	Dry		300–1200	0.1	313	−5.48	Zheng & Fu (1998)
Albite*	Ab	Wet	⊥(001)	350–800	100	89 ± 5	−18.89	Giletti *et al.* (1978)
Albite	Ab	Dry	Sphere	750–950	0.1	90	−36.15	Matthews *et al.* (1994)
Anorthite*	An	Wet	⊥(001)	350–800	100	110 ± 5	−15.79	Giletti *et al.* (1978)
Anorthite	An	Dry	⊥(001)	850–1300	0.1	236 ± 8	−11.51	Elphick *et al.* (1988)
Kyanite	Ky	Wet		300–1200	100	328	−4.42	Zheng & Fu (1998)
Kyanite	Ky	Dry		300–1200	100	522	5.71	Zheng & Fu (1998)
Enstatite	En	Wet		300–1200	100	236	−9.28	Zheng & Fu (1998)
Enstatite	En	Dry		300–1200	100	361	−2.87	Zheng & Fu (1998)
Jadeite	Jd	Wet		300–1200	100	264	−7.80	Zheng & Fu (1998)
Jadeite	Jd	Dry		300–1200	0.1	410	−0.25	Zheng & Fu (1998)
Omphacite	Omp	Wet		300–1200	100	246	−8.75	Zheng & Fu (1998)
Omphacite	Omp	Dry		300–1200	100	379	−1.91	Zheng & Fu (1998)
Diopside*	Di	Wet	//c	700–1200	100	226 ± 21	−13.41	Farver (1989)
Diopside*	Di	Dry		300–1200	0.1	329	−4.61	Zheng & Fu (1998)
Hornblende	Hb	Wet	//c	650–800	100	172 ± 25	−16.12	Farver & Giletti (1985)
Muscovite	Mus	Wet	powder	512–700	100	163 ± 21	−9.47	Farver & Giletti (1991)
Phlogopite	Phl	Wet	powder	600–900	100	176 ± 13	−8.87	Farver & Giletti (1991)
Biotite	Bi	Wet	powder	500–800	100	142 ± 18	−11.61	Farver & Giletti (1991)
Epidote	Ep	Wet		300–1200	100	230	−9.58	Zheng & Fu (1998)
Almandine*	Alm	Wet	isotropic	800–1000	100	301 ± 46	−9.72	Coghlan (1990)
Almandine	Alm	dry		300–1200	0.1	474	3.15	Zheng & Fu (1998)
Grossular	Grs	wet		300–1200	100	254	−8.31	Zheng & Fu (1998)
Grossular	Grs	dry		300–1200	0.1	394	−1.15	Zheng & Fu (1998)
Pyrope	Prp	wet		300–1200	100	311	−5.27	Zheng & Fu (1998)
Pyrope	Prp	dry		300–1200	0.1	494	4.20	Zheng & Fu (1998)
Zircon	Zr	wet	//c or ⊥c	767–1160	7–70	210	−16.72	Watson & Cherniak (1997)
Zircon	Zr	dry	//c or ⊥c	1100–1500	0.1	448	0.28	Watson & Cherniak (1997)
Titanite*	Tt	wet	//a,b,c	700–900	100	254 ± 28	−9.21	Morishita *et al.* (1996)
Titanite	Tt	dry		300–1200	0.1	306	−5.83	Zheng & Fu (1998)
Forsterite	Fo	wet		300–1200	100	230	−9.58	Zheng & Fu (1998)
Forsterite	Fo	dry		300–1200	0.1	352	−3.38	Zheng & Fu (1998)
Rutile	Rt	wet	//c	750–1000	100	330 ± 15	−0.53	Moore *et al.* (1998)

Rutile	Rt	dry	//c	750–1000	0.1–100	258 ± 22	−5.36	Moore *et al.* (1998)
Magnetite	Mt	wet		550–800	100	188	−12.56	Giletti & Hess (1988)
Magnetite	Mt	dry		300–1200	0.1	333	−4.39	Zheng & Fu (1998)
Ilmenite	Ilm	wet		300–1200	100	247	−8.70	Zheng & Fu (1998)
Ilmenite	Ilm	Dry		300–1200	0.1	381	−1.84	Zheng & Fu (1998)
Sr								
Calcite	Cc	dry	//(10$\bar{1}$4)	400–800	0.1	132 ± 6	−19.99	Cherniak (1997)
Albite	Ab	dry	⊥(001)	675–1025	0.1	224 ± 11	−10.45	Cherniak (1997)
Albite*	Ab	wet	//c	640–800	100	247 ± 25	−3.68	Giletti (1991)
Orthoclase	Or	dry	⊥(001)	725–1075	0.1	284 ± 7	−5.12	Cherniak & Watson (1992)
Orthoclase*	Or	wet	//c	625–900	100	167 ± 17	−16.12	Giletti (1991)
Anorthite	An	dry	//c	900–1300	0.1	267 ± 58	−9.77	Giletti & Casserly (1994)
Diopside*	Di	dry	//c	1100–1250	0.1	406 ± 71	3.99	Sneeringer *et al.* (1984)
Diopside*	Di	dry	//a	1100–1250	2000	259 ± 50	−10.98	Sneeringer *et al.* (1984)
Hornblende*	Hb	wet	//c	700–960	200	260 ± 12	−7.62	Brabander & Giletti (1995)
Phlogopite	Phl	dry		550–1250	0.1	145	−20.56	Hammouda & Cherniak (2000)
Muscovite*	Mus	wet		300–600	300	105	−25.43	Jenkin (1997)
Biotite*	Bi	wet	//c	500–900	100	100 ± 5	−21.98	Giletti (1991)
Almandine*	Alm	wet	isotropic	800–1000	100	205 ± 17	−18.42	Coghlan (1990)
Titanite*	Tt	wet	//c	700–900	100	234	−12.48	Morishita *et al.* (1990)
Titanite*	Tt	dry	//(100)	925–1175	0.1	415 ± 27	0.99	Cherniak (1995)
Fluorapative	Fap	dry	⊥c	700–1050	0.1	272 ± 9	−5.91	Cherniak & Ryerson (1993)
Fluorapative	Fap	wet	//c	650–1000	100	104	−24.64	Farver & Giletti (1989)
Sm–Nd								
Calcite	Cc	dry	powder	600–850	0.1	150 ± 14	−22.15	Cherniak (1998)
Oligoclase	An_{23}	dry	⊥(010)	925–1350	0.1	425	3.14	Cherniak (2003)
Labradorite	An_{67}	dry	⊥(010)	925–1350	0.1	477	5.48	Cherniak (2003)
Anorthite	An_{93}	dry	⊥(010)	925–1350	0.1	398	−2.83	Cherniak (2003)
Diopside*	Di	dry	⊥(001)	1050–1450	0.1	496 ± 77	2.42	Van Orman *et al.* (2001)
Diopside	Di	dry	//c	1100–1250	800	238 ± 46	−13.17	Sneeringer *et al.* (1984)
Diopside	Di	dry	//a	1100–1250	2000	197 ± 50	−15.94	Sneeringer *et al.* (1984)
Almandine	Alm	wet	isotropic	800–1000	100	184 ± 29	−19.59	Coghlan (1990)
Almandine	Alm	dry	isotropic	777–827	0.1	258	−9.97	Ganguly *et al.* (1998)
Pyrope*	Prp	dry	isotropic	1200–1450	2800	300 ± 30	−12.00	Van Orman *et al.* (2002)
Fluorapatite	Fap	dry	powder	1050–1250	0.1	218	−12.98	Watson *et al.* (1985)
Fluorapatite	Fap	dry	⊥c	750–1100	0.1	298 ± 17	−5.07	Cherniak (2000)
Zircon	Zr	dry	powder	1200–1400	0.1	841 ± 57	28.69	Cherniak *et al.* (1997)
Titanite*	Tt	dry	//(100)	925–1175	0.1	498 ± 29	7.85	Cherniak (1995)
Ar								
Orthoclase*	Or	wet	powder	500–800	200	180 ± 5	−4.62	Foland (1974)
Hornblende*	Hbl	wet	powder	750–900	100	268 ± 7	−3.73	Harrison (1981)
Phlogopite*	Phl	wet	powder	600–900	200, 1500	242 ± 11	−0.29	Giletti (1974)
Biotite*	Bt	wet	powder	600–750	100, 1400	197 ± 9	−2.56	Harrison *et al.* (1985)

*Asterisk after mineral name denotes the diffusion data used in plotting the Arrhenius relationship.

Wang *et al.* 1989; Xu *et al.* 1992), this region has been one of the most important targets for studying UHP metamorphism during continental subduction and collision. Many tectonic, petrologic, geochemical and geochronological studies have been devoted to UHP eclogites, gneisses, quartz schist and jadeite quartzite (e.g. Wang *et al.* 1995; Cong 1996; Liou *et al.* 1996). It has been the common consensus that the UHP metamorphism took place in the Triassic by northward subduction of the Yangtze plate underneath the North China plate (Fig. 3A). Anomalously low $\delta^{18}O$ values of -5 to $-2‰$ have been recovered from eclogites and associated gneisses in the UHP terrane, which are ascribed to ancient meteoric water–rock interaction at some time prior to the UHP metamorphism (Baker *et al.* 1997; Yui *et al.* 1997; Zheng *et al.* 1998, 1999, 2000, 2003; Fu *et al.* 1999; Xiao *et al.* 2000, 2002; Zhang *et al.* 2003). In this context, surface materials on the continental crust were carried into the mantle by plate subduction, and the recycled crust has been returned to the surface in the suture zone of a continent–continent collision.

The present study focuses on eclogite, garnet amphibolite, paragneiss and granitic orthogneiss from Shuanghe in the eastern part of the Dabie terrane (Fig. 3A). As shown by Cong *et al.* (1995) and Liou *et al.* (1997), the UHP metamorphic rocks at Shuanghe form an elongate tectonically bound slab, with a NNW–SSE trend, exposed over an area of about 1 km^2. Within the UHP slab the eclogite and paragneiss occur as compositional layers with marble and jadeite quartzite. It is divided by a dextral strike-slip strike fault into two slabs, which are surrounded by the granitic orthogneiss (Fig. 3B).

A number of studies of the petrographic features, mineral parageneses and compositions have been conducted for eclogites, gneisses and jadeite quartzite at Shuanghe (e.g. Okay 1993; Cong *et al.* 1995; Liou *et al.* 1997; Carswell *et al.* 2000). Paragenesis of the UHP rocks is as

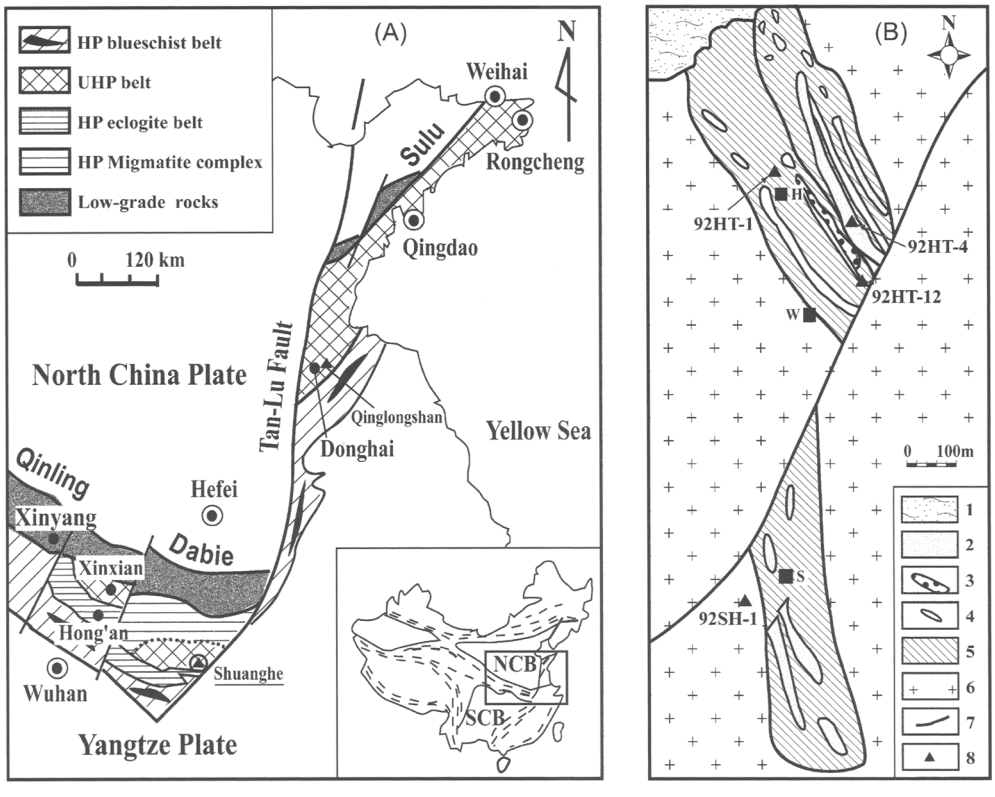

Fig. 3. Tectonic and geological maps of the Dabie–Sulu orogen and Shuanghe slab. (**A**) Sketch map of the geology of the Dabie–Sulu orogen. (**B**) Simplified geological map for metamorphic rocks at Shuanghe. Key: 1, granitic orthogneiss; 2, eclogite; 3, jadeitic quartzite; 4, marble; 5, biotite paragneiss (including micaceous schists); 6, mesozoic granite; 7, fault; 8, sample locality. H, W and S denote the villages of Hangjiacun, Wangdawu and Shuanghe, respectively.

follows: (1) eclogite: garnet + omphacite (Jd = 60) + rutile + quartz ± zoisite; (2) biotite paragneiss: garnet (almandine-rich) + phengite (Si = 3.4 to 3.6 pfu) + plagioclase (An = 16 to 29) + epidote + rutile/titanite + biotite; (3) granitic orthogneiss: garnet (high spessartine, low pyrope) + phengite (Si = 3.21 to 3.35 pfu) + plagioclase (An = 3 to 11) + K-feldspar + epidote + biotite; (4) garnet amphibolite: garnet + amphibole + titanite + sodic plagioclase + quartz + apatite. The UHP index minerals have been identified in the eclogite, biotite paragneiss and granitic orthogneiss at this locality (Cong *et al.* 1995; Liu *et al.* 2001). Therefore, the different types of mafic and felsic rocks all experienced the same geodynamic processes and thus were part of a single tectonic entity throughout the course of subduction, UHP metamorphism and exhumation.

Three metamorphic stages have been recognized for the UHP rocks at Shuanghe (Okay 1993; Cong *et al.* 1995; Liou *et al.* 1997; Carswell *et al.* 2000; Zhang *et al.* 2003): (1) Peak UHP eclogite facies, which is recorded by coesite and jadeite-rich omphacite inclusions in garnet. Metamorphic temperatures range from 720 to 880 °C at >2.8 GPa. (2) HP eclogite-facies recrystallization, which is represented by the coexistence of garnet and omphacite with quartz instead of coesite. Metamorphic conditions were estimated to be 630 to 760 °C and 1.3 to 1.6 GPa. (3) Amphibolite-facies retrogression, which is indicated by the occurrence of various symplectites such as amphibole + sodic plagioclase but the disappearance of omphacite from eclogite. Temperature and pressure conditions were estimated to be 470 to 570 °C and 600 to 800 MPa.

Geochronology

Detailed U–Pb, Sm–Nd and Rb–Sr isotopic dating studies have already been carried out for the eclogites, biotite paragneiss, granitic orthogneiss and jadeite quartzite at Shuanghe (Li *et al.* 1997, 2000; Chavagnac *et al.* 2001; Ayers *et al.* 2002; Zheng *et al.* 2003). Zircon U–Pb dating by means of a Wetherill-type discordia approach yielded lower intercept ages of 237 ± 4 and 233 ± 21 Ma for the biotite paragneiss (Fig. 4A and B), and 228 ± 12 and 226 ± 8 Ma for the granitic orthogneiss. Mineral Sm–Nd isochron dating gave ages of 226 ± 3 and 242 ± 3 Ma for the eclogites 227 ± 2, 231 ± 35 and 246 ± 2 Ma for the biotite paragneiss, and 213 ± 5 Ma for the granitic orthogneiss. Mineral Rb–Sr isochron dating yielded ages of 174 ± 8 Ma for the eclogite, 167 ± 3 to 202 ± 6 Ma for the biotite paragneiss, and 171 ± 3 and 173 ± 3 Ma for the granitic orthogneiss. Along with the radiometric dating for UHP metamorphic rocks in the other areas of the Dabie terrane (Li *et al.* 1999), it appears that the UHP metamorphism at Shuanghe also took place in the Triassic, but suffered amphibolite-facies retrogression in the Early Jurassic.

Oxygen isotope analysis presented in this study (Table 3) has used the mineral aliquots of the Shuanghe samples for the Sm–Nd and Rb–Sr radiometric dating (Li *et al.* 2000), including one paragneiss, one granitic orthogneiss, one eclogite and one garnet amphibolite. The sample locations are shown in Figure 3B, and their petrology is briefly summarized as follows.

(1) *Paragneiss* (92HT-1) is interlayered with marble containing eclogite nodules and mainly consists of quartz, garnet, epidote, biotite, phengite and plagioclase with minor titanite and rutile. Phengite is partially replaced by biotite and rutile by titanite.

(2) *Granitic orthogneiss* (92SH-1) belongs to regional country rocks enclosing the eclogite and paragneiss. It is mainly composed of quartz, K-feldspar, plagioclase, biotite, epidote and garnet (high spessartine of 18.6 to 34.9 mol% but low pyrope of 1.0 to 3.8 mol%).

(3) *Eclogite* (92HT-4) is fined-grained and massive, and mainly consists of garnet, omphacite, rutile and quartz with minor amphibole. Relict coesite, or its pseudomorph, was observed as inclusions in garnet.

(4) *Garnet amphibolite* (92HT-12) is a retrograded eclogite occurring as a nodule in the marble and composed of quartz, calcite, garnet, amphibole, plagioclase and titanite with minor apatite and zircon. Except for omphacite inclusions in garnet, all the omphacite has been retrograded to amphibole, but no biotite was observed. Recrystallized quartz and apatite coexisting with amphibole and titanite are common. In addition, titanite occurs as a corona around ilmenite that contain relicts of rutile.

As shown in Figure 5A–D, mineral Sm–Nd isochron dating yields consistent Triassic ages of 227 ± 2 Ma (246 ± 2 Ma) 213 ± 5 Ma, 226 ± 3 Ma and 238 ± 3 Ma, respectively. This demonstrates that Sm–Nd isotope equilibrium in these rocks was achieved in the Triassic during UHP and HP eclogite-facies metamorphism and preserved afterwards without significant

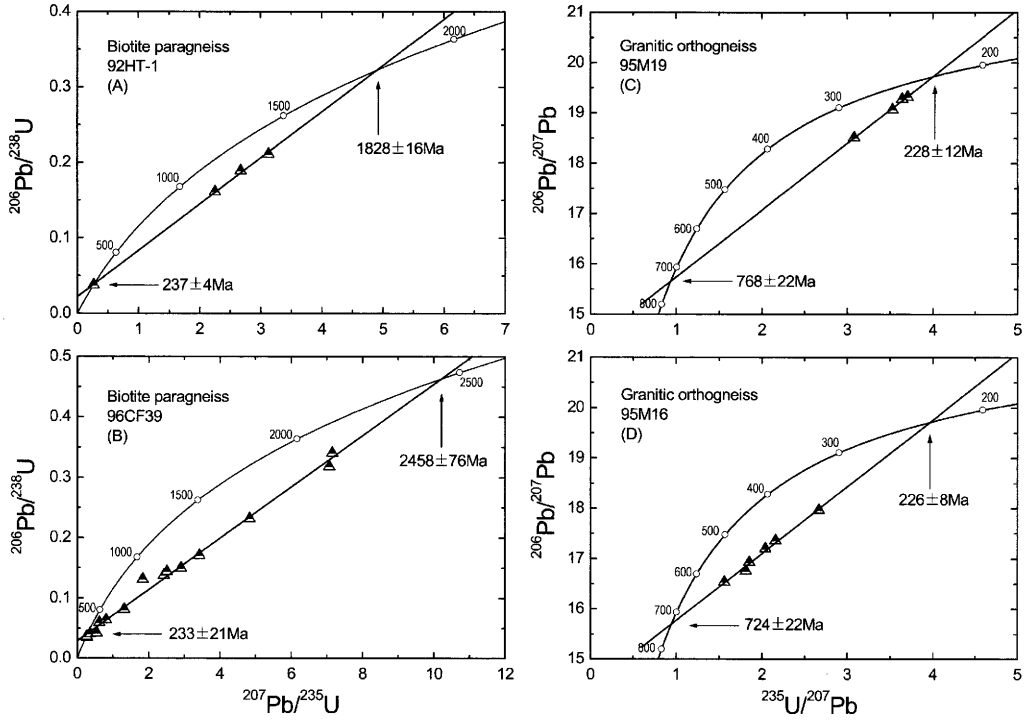

Fig. 4. U–Pb discordia diagrams for zircons from UHP gneisses at Shuanghe in the Dabie terrane. (**A**, **B**) Biotite paragneiss on conventional Wetherill-type concordia diagram in the space of $^{206}Pb/^{238}U$ v. $^{207}Pb/^{235}U$ (data after Li *et al.* 1997; Chavagnac *et al.* 2001). (**C**, **D**) Granitic orthogneiss in a plot of $^{206}Pb/^{207}Pb$ v. $^{235}U/^{207}Pb$ (data after Zheng *et al.* 2003). The advantage of the modified concordia diagram is that its concordia curve is expanded relative to the conventional one at later times (<1000 Ma), and thus a stronger curvature of the concordia curve is obtained to better show the intersection relationship between the discordia line and the concordia curve for the samples having Neoproterozoic and Phanerozoic ages (Zheng 1990, 1992*b*).

disturbance. However, the symplectite assemblage of amphibole + titanite + apatite in sample 92HT-12 gives an Sm–Nd isochron age of 200 ± 23 Ma (inset in Fig. 5D), pointing to disturbance of mineral Sm–Nd system by later amphibolite-facies recrystallization.

On the other hand, mineral Rb–Sr isochron dating for these same samples yields consistent ages of 174 ± 4 Ma, 171 ± 3 Ma and 174 ± 8 Ma (Fig. 6A, B and D, respectively). This implies that the Rb–Sr isotope systems in the UHP rocks were completely reset at the beginning of the Middle Jurassic by amphibolite-facies retrogression to achieve isotopic re-equilibration. Only one phengite–garnet Rb–Sr isochron gives a Triassic age of 219 ± 7 Ma for the paragneiss 92HT-1 (inset in Fig. 6A), pointing to preservation of the Rb–Sr chronometric signature in the two refractory minerals since the HP eclogite-facies recrystallization. The same was observed in the eclogite at Qinglongshan in western Sulu, where mineral Rb–Sr and Sm–Nd isochrons yield nearly consistent Triassic ages of 220 ± 1 Ma (Fig. 6C) and 226 ± 5 Ma (Li *et al.* 1994). The integrated U–Pb, Sm–Nd and Rb–Sr ages suggest that continuous isotopic resetting during HP eclogite-facies recrystallization probably ceased at about 225 ± 5 Ma and continuous isotopic resetting during amphibolite-facies retrogression ceased at about 175 ± 5 Ma.

Oxygen isotopes

Oxygen isotope analysis was carried out using the laser fluorination technique of Sharp (1990) using a 25 W MIR-10 CO_2 laser at Hefei (Zheng *et al.* 2002). O_2 was directly transferred to the Delta$^+$ mass spectrometer for the measurement of $^{18}O/^{16}O$ and $^{17}O/^{16}O$ ratios (Rumble *et al.* 1997). Oxygen isotope data are reported as parts per thousand differences (‰) from the reference standard VSMOW in the $\delta^{18}O$ notation. Two reference minerals were used: $\delta^{18}O = 5.8‰$ for

Table 3. *Oxygen isotope composition of minerals and estimated temperatures*

Sample		$\delta^{18}O$ (‰)	Pair*	$\Delta^{18}O$ (‰)	T (°C)†
92HT-1	Quartz	12.44			
Paragneiss	Phengite	9.83	Qz–Phg	2.61	600
	Biotite	7.42	Qz–Bi	5.02	510
	Garnet	8.51	Qz–Gt	3.93	645
	Whole-rock	10.6			
92SH-1	Quartz	−0.43			
Granitic	Plagioclase	−2.71	Qz–Pl	2.28	420
orthogneiss	Epidote	−5.02	Qz–Ep	4.59	430
	Biotite	−6.90	Qz–Bi	6.47	410
	Garnet	−4.51	Qz–Gt	4.08	630
	Whole-rock	−3.4			
92HT-4	Quartz	8.87			
Eclogite	Omphacite	6.46	Qz–Omp	2.41	700
	Garnet	5.58	Qz–Gt	3.29	730
	Rutile	2.09	Qz–Rt	6.82	520
	Whole-rock	5.9			
92HT-12	Quartz	15.43			
Garnet	Plagioclase	13.54	Qz–Pl	1.89	500
amphibolite	Amphibole	11.18	Qz–Hb	4.25	550
	Garnet	7.47	Qz–Gt	7.96	<400
	Titanite	11.65	Qz–Tt	3.78	720
	Whole-rock	11.7			

*Mineral abbreviations: Bi, biotite; Ep, epidote; Gt, garnet; Hb, amphibole; Omp, omphacite; Phg, phengite; Pl, plagioclase (An = 10); Qz, quartz; Tt, titanite.
†Calculated using the calibration listed in Table 1.

UWG-2 garnet (Valley *et al.* 1995), and $\delta^{18}O = 5.2‰$ for SCO-1 olivine (Eiler *et al.* 1995). Reproducibility for repeat measurements of each standard on a given day was better than $\pm 0.1‰$ (1σ) for $\delta^{18}O$. Table 3 lists the analysed results on individual minerals and whole rock from the UHP rocks at Shuanghe.

The isotherm diagram is a graphical approach to illustrate the oxygen isotope fractionations between quartz and the other minerals as a function of temperature. As shown in Figure 7, O isotope geothermometry on the paragneiss, granitic orthogneiss, eclogite and garnet amphibolite at Shuanghe yields two sets of temperature, the first at 720 to 600 °C and the second at 540 to 420 °C. Compared to the known metamorphic conditions from the petrologic thermometers (Okay 1993; Cong *et al.* 1995; Liou *et al.* 1997; Carswell *et al.* 2000), the first set may correspond to the preservation of HP eclogite-facies temperatures in the refractory minerals during exhumation, and the second set to isotopic resetting in the hydroxyl-bearing minerals due to amphibolite-facies retrogression.

For paragneiss 92HT-1 (Fig. 7A), the O isotope temperatures of 600 to 645 °C for phengite and garnet correspond to HP eclogite-facies conditions during cooling, but the amphibolite-facies retrogression has reset the oxygen isotope system in biotite to yield the low temperature of 510 °C. Biotite has faster rates of oxygen diffusion relative to garnet and phengite (Table 2) and thus is easily susceptible to oxygen isotope resetting.

For granitic orthogneiss 92SH-1 (Fig. 7B), it appears that the retrograde minerals such as plagioclase, biotite and epidote give consistent temperatures of 410 to 430 °C when paired with quartz, suggesting oxygen isotope re-equilibration during amphibolite-facies recrystallization. Nevertheless, O isotope geothermometry concerning garnet in this sample gives a temperature of 630 °C, indicating the preservation of HP eclogite-facies temperatures during exhumation because garnet has much slower rates of oxygen diffusion relative to plagioclase, biotite and epidote (Table 2).

For eclogite 92HT-4 (Fig. 7C), the O isotope temperature of 700 to 730 °C for omphacite and garnet suggests preservation of the UHP conditions in the refractory assemblage despite the amphibolite-facies retrogression that has yielded the low temperature of 520 °C for rutile. Rutile is a mineral that not only has fast rates of oxygen diffusion relative to garnet and pyroxene (Table 2) but also is easily subject to retrograde recrystallization, so that it has low closure temperatures of oxygen diffusion.

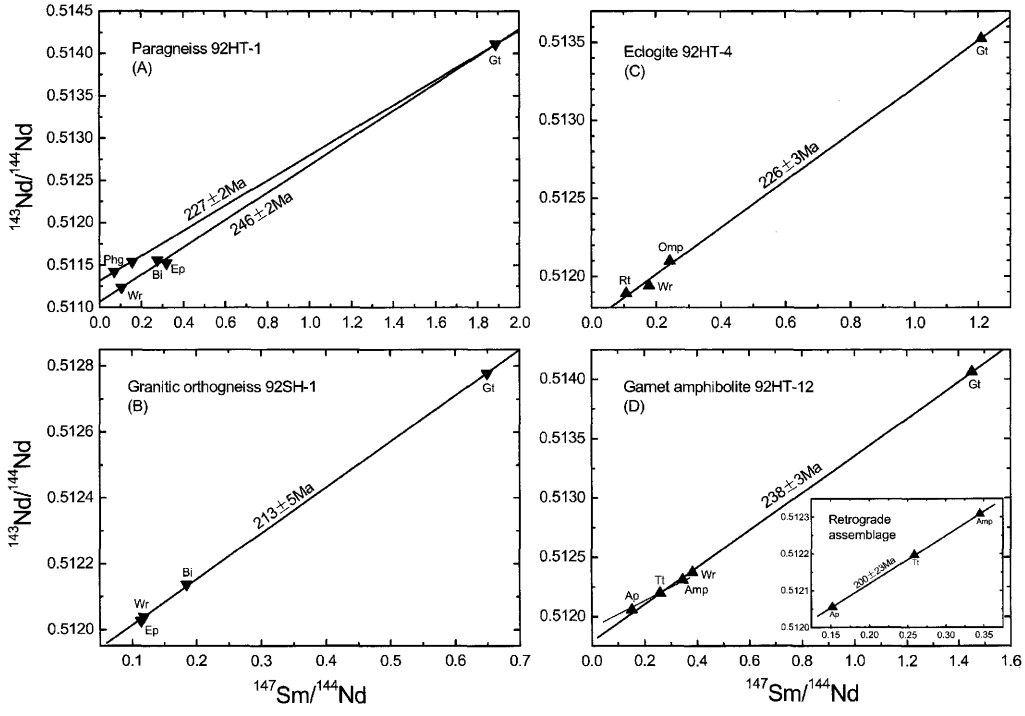

Fig. 5. Mineral Sm–Nd isochron plot for paragneiss, granitic orthogneiss, eclogite and garnet amphibolite from Shuanghe in the Dabie terrane (data after Li *et al.* 2000).

For garnet amphibolite 92HT-12 (Fig. 7D), it appears that garnet is in isotopic disequilibrium with the other minerals because of the following observations (Table 3): (1) the measured fractionations between quartz, plagioclase, amphibole and garnet are too large to be in equilibrium with each other (refer to Table 1); (2) the measured fractionation between garnet and titanite is negative, which is opposite to the sequence of ^{18}O enrichment at thermodynamic equilibrium (refer to Table 1); (3) the unreasonably low oxygen isotope temperature of less than 400 °C for the quartz–garnet pair, which is at odds with the slow rate of oxygen diffusion in garnet (refer to Table 2) that should yield a high oxygen isotope temperature. Obviously, the garnet is a relict mineral from the precursor eclogite, whereas the other minerals are new symplectites formed by the amphibolite-facies retrogression. Nevertheless, titanite, amphibole and plagioclase give decreasing closure temperatures of 720, 550 to 500 °C, respectively, when paired with quartz, suggesting differential resetting of oxygen isotopes by retrograde exchange during slow cooling from the HP eclogite-facies to the amphibolite-facies conditions.

Whole-rock $\delta^{18}O$ values for the paragneiss and the granitic orthogneiss from Shuanghe are +10.6% (Fig. 7A) and −3.4‰ (Fig. 7B), respectively; those for the eclogites and garnet amphibolite from Shuanghe are +5.9‰ (Fig. 7C) and +11.7‰ (Fig. 7D), respectively. The low $\delta^{18}O$ value of −3.4, with the equilibrium fractionations among the UHP minerals, suggests pre-subduction meteoric–hydrothermal alteration at high temperatures. In fact, the presence of a H_2O-rich fluid is evident in the protolith of the gneisses and amphibolite at Shuanghe, as indicated by the occurrence of hydroxyl-bearing minerals. On the other hand, the high $\delta^{18}O$ values of +11.7 to +5.9‰, with the equilibrium fractionations among the UHP minerals, from the paragneiss, eclogite and garnet amphibolite at Shuanghe does not rule out pre-subduction water–rock interaction for their sedimentary protoliths. Because sedimentary rocks can have $\delta^{18}O$ values as high as +15 to +25‰ (Hoefs 1997), their $\delta^{18}O$ values may have decreased by 10 to 15‰ by the same meteoric–hydrothermal alteration. In either case, the fluid is an important medium to promote Nd, Sr and O isotopic equilibrium by intragranular and intergranular

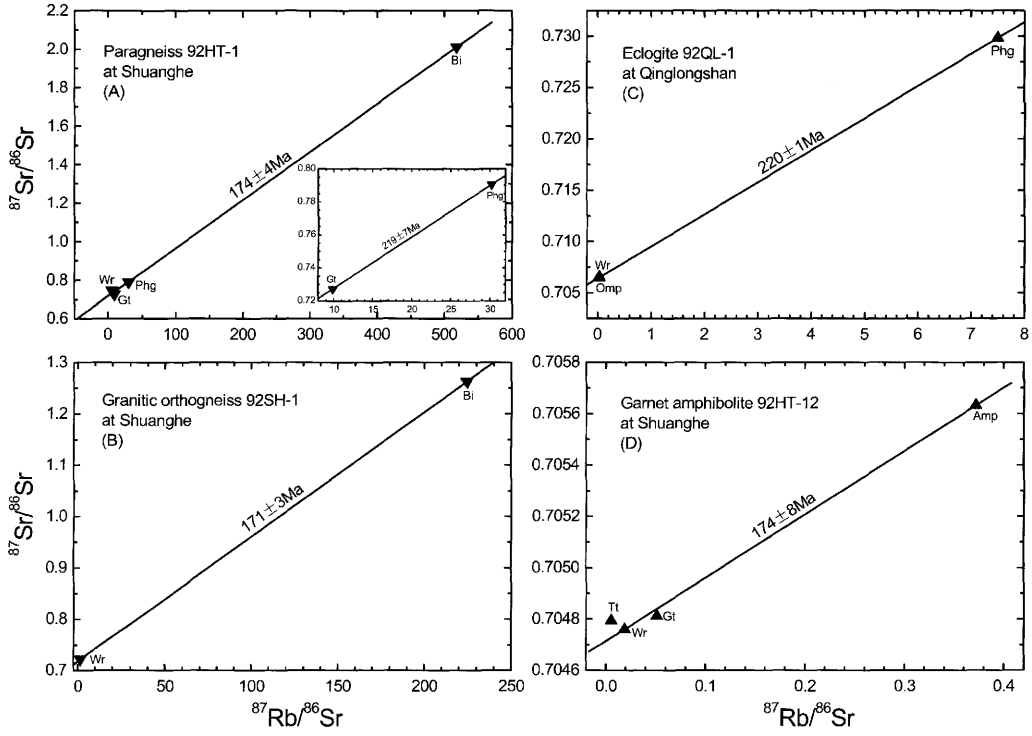

Fig. 6. Mineral Rb–Sr isochron plot for paragneiss, granitic orthogneiss and garnet amphibolite from Shuanghe in the Dabie terrane (data after Li *et al.* 2000). Eclogite from Qinglongshan in the Sulu terrane is shown for comparison (data after Li *et al.* 1994).

diffusion among the felsic and mafic minerals during the peak UHP metamorphism and the subsequent HP eclogite-facies recrystallization.

Discussion

The mineral Rb–Sr isochron ages of 174 ± 8 to 171 ± 3 Ma for the two gneisses and one amphibolite from Shuanghe are interpreted to date the timing of cessation of amphibolite-facies retrogression at about 540 to 420 °C. The preservation of Triassic Sm–Nd isochron ages for the same samples (Fig. 5A, B and D) implies faster rates of Sr diffusion than Nd diffusion among the UHP minerals on the scale of a hand-specimen during the amphibolite-facies metamorphism. Paragneiss 92HT-1 was strongly retrogressed at the amphibolite-facies conditions, but the partially retrograded assemblage of Gt + Ep + Bi + Wr still defines a statistically valid Sm–Nd isochron age of 246 ± 2 Ma (Fig. 5A). This indicates less REE mobility than Sr and O during the retrograde metamorphism. It is known that garnet, phengite and biotite have significantly different rates of Sr diffusion, but the Rb–Sr isotope data for the Bi–Phg–Gt–Wr assemblage from paragneiss 92HT-1 still define the statistically valid isochron age of 174 ± 4 Ma (Fig. 6A). This indicates rapid cooling from 500 °C subsequent to the amphibolite-facies retrogression. However, the Phg–Gt Rb–Sr system (inset in Fig. 6A) may be closed at about 600 °C (Fig. 7A) and 219 ± 7 Ma since the HP eclogite-facies recrystallization. This implies that closure temperature of Sr diffusion in phengite is higher than that in biotite.

Preservation of eclogite-facies Sm–Nd isotope equilibrium between garnet and omphacite in eclogite 92HT-4 is evident, as indicated by the Triassic age of 226 ± 3 Ma (Fig. 5C) in combination with the sensible O isotope temperature of 720 °C (Fig. 7C). A similar case was observed for the eclogite at Qinglongshan in the Sulu terrane (Zheng *et al.* 2002), where the O isotope temperatures of 700 to 800 °C are correlated with the reasonably concordant Sm–Nd and Rb–Sr isochron ages of 226 ± 5 Ma and 220 ± 1 Ma (Li *et al.* 1994). This suggests that the closure temperature of Sr diffusion in

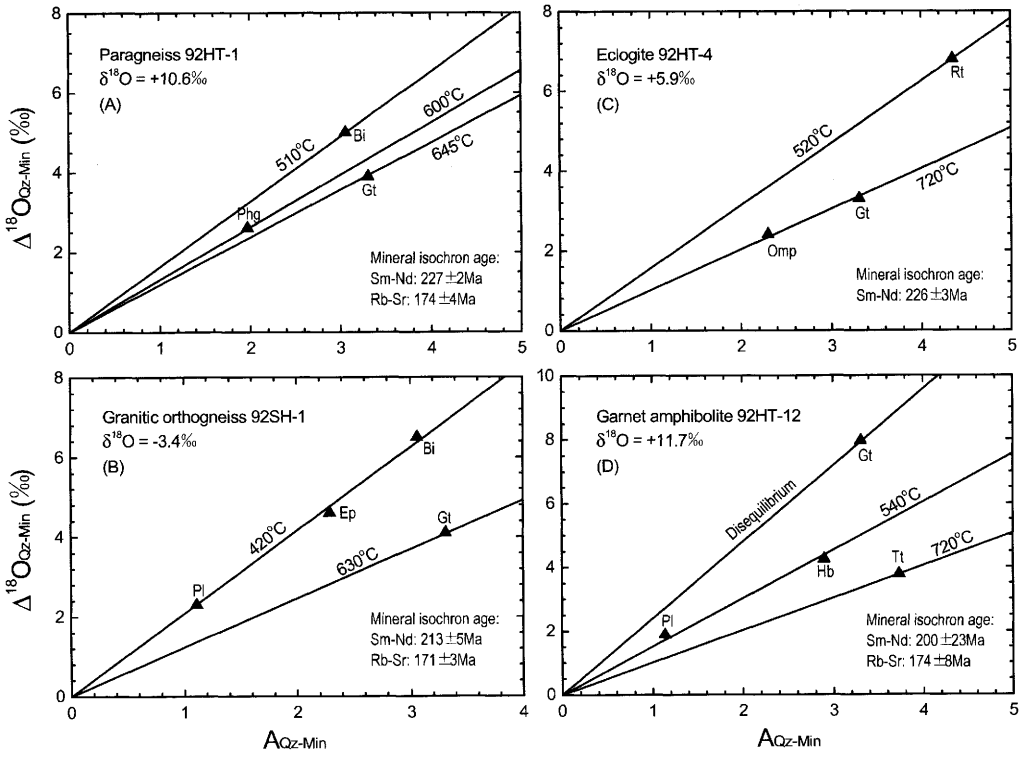

Fig. 7. Isotherm plot for oxygen isotope fractionations between quartz and the other minerals from paragneiss, granitic orthogneiss, eclogites and garnet amphibolite at Shuanghe in the Dabie terrane (data after Table 3). Parameters $A_{Qz\text{-}Min}$ refer to temperature coefficients in oxygen isotope fractionation equations for quartz–mineral pairs in the form of $10^3 \ln\alpha = A \times 10^6/T^2$ (after Table 1).

phengite may be lower than, but close to, that of Nd diffusion in garnet.

Garnet amphibolite 92HT-12 was derived from strongly retrograded eclogite at the amphibolite-facies conditions. The residual and retrograded assemblage of Gt + Amp + Tt + Ap + Wr yields a Sm–Nd isochron age of 238 ± 3 Ma (Fig. 5D), whereas the Amp–Wr assemblage gives a Rb–Sr isochron age of 174 ± 8 Ma (Fig. 6D). O isotope re-equilibration has been achieved among the newly crystallized minerals (Fig. 7D), yielding the reset temperatures of 540 and 500 °C for quartz–hornblende and quartz–plagioclase pairs, respectively. These suggest a limited mobility of REE in a relatively closed system during the amphibolite-facies retrogression, but much larger mobilities of Sr and O under the same metamorphic conditions. The Sr and O isotopic disequilibria between the residual garnet and the newly grown minerals are significant, as indicated by the downward deviation of the garnet data point from the isochron (Fig. 6D) and the unreasonably low temperature (Fig. 7D).

Although the Sm–Nd isochrons give consistent Triassic ages of 213 to 238 Ma for UHP metamorphism, the Rb–Sr isochrons give Jurassic ages of 171 to 174 Ma for the same samples. O isotope geothermometry of the gneiss, eclogite and amphibolite minerals yields two sets of temperature of 600 to 720 °C and 420 to 540 °C, respectively, corresponding to cessation of continuous isotopic resetting at about 225 ± 5 Ma during HP eclogite-facies recrystallization and that at about 175 ± 5 Ma during amphibolite-facies retrogression (Fig. 8). The preservation of the Triassic Sm–Nd isochron ages, but the occurrence of the Jurassic Rb–Sr isochron ages and the regular O isotope temperatures for the same samples, suggest faster rates of Sr and O diffusion relative to Nd diffusion among the UHP minerals on hand-specimen scale during the amphibolite-facies retrogression. This is consistent with experimental data that diffusion rates of trivalent cations (e.g. REE) are much slower than diffusion rates of divalent cations (e.g. Ca, Mg or Fe) in the

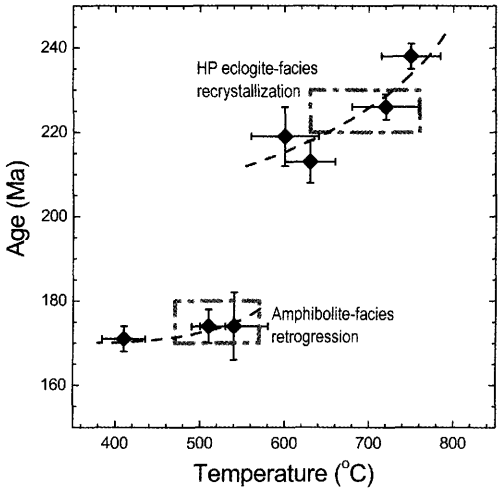

Fig. 8. Relationship between oxygen isotope temperature and isochron age for metamorphic minerals from paragneiss, granitic orthogneiss, eclogites and garnet amphibolite at Shuanghe in the Dabie terrane. Although the closure temperatures of oxygen diffusion do not simply correspond to those of Sr or Nd diffusion, O, Sr and Nd isotopic resetting is evident by two episodes of metamorphism in the Late Triassic and at the beginning of Middle Jurassic, respectively.

same minerals (Chakraborty & Ganguly 1992; Freer & Edwards 1999; Cherniak 2003; Van Orman *et al.* 2002). Experimental studies also show contrasting effects by pressure change: rates of Sm–Nd diffusion in diopside and almandine decrease with increasing pressure (Sneeringer *et al.* 1984; Ganguly *et al.* 1998; Van Orman *et al.* 2001), whereas rates of Sr and O diffusion in silicate minerals increase with increasing pressure (Sneeringer *et al.* 1984; Giletti 1985). Since the rates of Sr and O diffusion may respond differently to pressure change, Sr diffusion may become faster than O diffusion in metamorphic minerals during plate exhumation.

In general, mineral Sm–Nd or Rb–Sr isochrons for HP to UHP metamorphic rocks are constructed by two to three minerals (sometimes including whole rock); so are oxygen isotope geothermometers. It is critical to test whether the isotopic systems of interest have achieved and preserved isotopic equilibrium among isochron minerals at the time of their formation when evaluating the validity of either mineral Sm–Nd or Rb–Sr isochrons or O isotope geothermometry. In particular, it is essential to know which mineral has exerted the predominant control on isotopic re-equilibration among the isochron minerals and thus on the initiation of the isochron clock. While the mineral with slow diffusivity has exerted the primary control on the rate of isotope homogenization during metamorphism, the mineral with high parent/daughter (P/D) ratio has exerted the principal control on initiation of the isochron clock in response to metamorphic resetting. If the mineral with high P/D ratio has a fast rate of radiogenic isotope diffusion, a statistically valid isochron can be obtained to date the timing of the metamorphic event. In contrast, if the mineral with high P/D ratio has a slow rate of radiogenic isotope diffusion, no new isochron can be expected in response to the timing of the metamorphic resetting. It appears that the degree of isochron resetting depends on the degree and duration of the metamorphic event as well as the mobility of radiogenic isotopes among the metamorphic minerals (Zheng 1989).

The present case study on the Shuanghe UHP metamorphic rocks shows that the low apparent rate of Nd isotope re-equilibration among isochron minerals is due to the control exerted by garnet which has a high Sm/Nd ratio (Fig. 5) but a slower rate of Sm–Nd diffusion than Sr diffusion (Fig. 2). In contrast, the high apparent rate of Sr isotope re-equilibration reflects the high apparent rates of Sr transport in such hydroxyl-bearing minerals as biotite and hornblende that have not only high Rb/Sr ratios (Fig. 6) but also faster rates of Sr diffusion than the other minerals (Fig. 2). Nevertheless, the preservation of Triassic ages for Rb–Sr isochrons involving phengite from paragneiss (inset in Fig. 6A) and eclogite (Fig. 6C) suggests that the rate of Sr diffusion in phengite is slower than that in biotite and hornblende, but it is faster than, or close to, the rate of Nd diffusion in garnet. Because the mineral with high parent/daughter ratio has exerted the primary control on the construction of mineral Sm–Nd or Rb–Sr isochron chord, the difference between Nd and Sr diffusivities in this mineral dictates the degree of isochron resetting by the later geological event.

The present study provides insight into the kinetics of isotopic disequilibrium in the mineral chronometric systems of metamorphic rocks. Triassic ages of the mineral Sm–Nd and Rb–Sr isochrons were obtained for the eclogitic and gneissic minerals if O isotope equilibrium between cogenetic minerals is attained and preserved under HP eclogite-facies conditions. In contrast, Jurassic ages of the mineral Rb–Sr isochrons were obtained in the minerals when low O isotope temperatures of 540 to 420 °C are calculated due to the amphibolite-facies retrograde metamorphism. These observations can be reasonably interpreted in terms of the

difference between Nd, Sr and O diffusivities in the isochron minerals (Fig. 2). According to the experimentally determined diffusion coefficients, the rates of O diffusion in feldspars and micas are greater than those of Sr diffusion at high temperatures (Fig. 2E and F). As a result, attainment of Sr isotopic equilibrium in feldspar–mica systems suggests achievement of O isotopic equilibrium in the same systems. Likewise, preservation of O isotope equilibrium in the feldspar–mica systems implies the preservation of Rb–Sr isotope equilibrium in the same systems.

Similarly, the rates of O in garnet are faster than those of Nd diffusion but lower than those of Sr diffusion at the same temperatures (Fig. 2B); the rates of O and Sr diffusion in pyroxene are identical but consistently much faster than those of Nd diffusion at the same temperatures (Fig. 2C). As a result, attainment of O isotopic equilibrium in omphacite–garnet systems suggests achievement of Sr isotopic equilibrium in the same systems. Likewise, preservation of O isotope equilibrium in the omphacite–garnet systems implies the preservation of both Sm–Nd and Rb–Sr isotopic equilibrium in the same systems. Therefore, a combined study of stable and radiogenic isotopes in coexisting minerals provides powerful tools for clarifying the confusion concerning the interpretation of mineral Sm–Nd or Rb–Sr isochrons.

Conclusions

Isotopic equilibrium or disequilibrium is a crucial issue in identifying the validity of mineral isochron dating and geothermometry. Not only is the attainment of isotopic equilibrium during geological processes not always synchronous with mineralogical equilibration, but also the equilibria for different isotope systems in the same minerals do not exactly correspond to each other due to the difference in element diffusivity. Both isotopic equilibrium and disequilibrium are possible between metamorphic minerals, between accessory mineral inclusions and host mineral, between mineral cores and rims, and between altered product and precursor matrix during prograde, peak and retrograde metamorphism. The question is how to recognize the equilibrium or disequilibrium of chronometric systems in metamorphic minerals when the mineral isochron ages are applied to the tectonic evolution of metamorphic terranes, i.e. reasonable interpretation of radiometric clocks.

Mineral Sm–Nd, Rb–Sr and O isotope systems in UHP metamorphic rocks are often in partial equilibrium: equilibrium with respect to some minerals and isotopes, but not all. Because the isotope systems are subject to substantially different rates of intragranular and intergranular diffusion (Fig. 2), the integrated radiogenic and stable isotope data suggest that the equilibration of different isotope systems in minerals occurs over geologically different scales of time and length. For mineral Rb–Sr and Sm–Nd isochron dating, the isotopic equilibration means that the dated minerals have the same initial $^{87}Sr/^{86}Sr$ and $^{143}Nd/^{144}Nd$ ratios at the time of their formation (Zheng 1989). This corresponds to given oxygen isotope fractionations between the isochron minerals at equilibrium temperatures (Zheng *et al.* 2002). Kinetics of intragranular and intergranular diffusion of elements is the rate-limiting factor in high-T geological processes. The difference in the initial $^{87}Sr/^{86}Sr$ and $^{143}Nd/^{144}Nd$ ratios may be viewed as the gradient in chemical potential among different mineral grains. During metamorphism, rapid diffusion may flatten the intergranular chemical potential gradients for some elements (e.g. Sr), whereas slow diffusion for others preserves steep or intermediate gradients (e.g. Nd). As a result, the Rb–Sr isotope system in metamorphic rocks has equilibrated among minerals while the Sm–Nd isotope system has not with respect to a given scale of time and length.

The preservation of Triassic Sm–Nd isochron ages, but the occurrence of Jurassic Rb–Sr isochron ages and the regular O isotope temperatures for the same samples of UHP metamorphic rocks at Shuanghe in the Dabie terrane, suggest that rates of Sr and O diffusion in such hydroxyl-bearing minerals as biotite and hornblende are faster than rates of Nd diffusion in garnet and Sr diffusion in phengite on the scale of a hand-specimen during the amphibolite-facies retrogression. This indicates that there has been no resolvable transport of Sm–Nd since the time of HP eclogite-facies recrystallization, but significant exchange of Rb–Sr occurred some 50 Ma after Sm–Nd due to amphibolite-facies retrogression. While the mineral with high parent/daughter ratio has exerted the primary control on the construction of the mineral Sm–Nd or Rb–Sr isochron chord and thus on initiation of the isochron clock, the difference between Nd and Sr diffusivities in this mineral dictates the extent of isochron resetting during retrograde metamorphism. Therefore, in a rock that has experienced high temperatures and that contains phases with different closure temperatures and different grain sizes, complete diffusional re-equilibration can be expected, in which case a statistically valid isochron can be obtained if there exists a phase with much faster

rates of radiogenic isotope diffusion than other phases.

With respect to the interpretation of mineral isochron ages in connection with the closure temperatures of radiogenic isotope diffusion and the timescale of metamorphic processes, caution must be exercised not only because there are considerable differences in REE and Sr diffusivity among the isochron minerals (Fig. 2), but also because diffusion-controlled isotope exchange proceeds continuously in the courses of peak metamorphism, transition from peak to retrograde metamorphism, and retrograde metamorphism. In general, the mineral that has the fastest rate of diffusion exerts the primary control on initiation of the radiometric clock for isochron minerals and thus places the minimum estimates of timing and closure temperature for isotope resetting during a given geological process, whereas the mineral with the slowest rate of diffusion provides the maximum estimates. Therefore, a mineral isochron age may date a time–temperature point at which the geological process has just ended and thus retrograde isotope exchange has effectively ceased among the minerals during cooling to a given closure temperature.

This study was supported by funds from the Natural Science Foundation of China (40033010) and the Chinese Academy of Sciences (KZCX2-107). Thanks are due to B. Luais, D. P. Mattey and D. Vance for their reviews that helped the clarification of some ambiguities.

References

AGRINIER, P. 1991. The natural calibration of $^{18}O/^{16}O$ geothermometers: application to the quartz-rutile mineral pair. *Chemical Geology*, **91**, 49–64.

AYERS, J. C., DUNKLE, S., GAO, S. & MILLER, C. E. 2002. Constraints on timing of peak and retrograde metamorphism in the Dabie Shan ultrahigh-pressure metamorphic belt, east-central China, using U–Th–Pb dating of zircon and monazite. *Chemical Geology*, **186**, 315–331.

BAKER, J., MATTHEWS, A., MATTEY, D., ROWLEY, D. & XUE, F. 1997. Fluid-rock interactions during ultra-high pressure metamorphism, Dabie Shan, China. *Geochimica et Cosmochimica Acta*, **61**, 1685–1696.

BECKER, R. H. & CLAYTON, R. N. 1976. Oxygen isotope study of a Precambrian banded iron formation, Hamersley Range, western Australia. *Geochimica et Cosmochimica Acta*, **40**, 1153–1166.

BIRD, M., LONGSTAFFE, F. J. & FYFE, W. S. 1993. Oxygen-isotope fractionation in titanium-oxide minerals at low temperatures. *Geochimica et Cosmochimica Acta*, **57**, 3083–3091.

BOTTINGA, Y. & JAVOY, M. 1975. Oxygen isotope partitioning among minerals in igneous and metamorphic rocks. *Reviews in Geophysics and Space Physics*, **13**, 401–418.

BRABANDER, D. J. & GILETTI, B. J. 1995. Strontium diffusion kinetics in amphiboles and significance to thermal history determinations. *Geochimica et Cosmochimica Acta*, **59**, 2223–2238.

BRADY, J. B. 1995. Diffusion data for silicate minerals, glasses, and liquids. *In:* AHRENS, T. J. (ed.) *Mineral Physics and Crystallography*. AGU Reference Shelf, **2**, Washington DC, 269–290.

BRUECKNER, H. K., BLUSZTAJN, J. & BAKUN-CZUBAROW, N. 1996. Trace element and Sm–Nd 'age' zoning in garnets from peridotites of the Caledonian and Variscan Mountains and tectonic implications. *Journal of Metamorphic Geology*, **14**, 61–73.

BURTON, K. W., KOHN, M. J., COHEN, A. S. & O'NIONS, R. K. 1995. The relative diffusion of Pb, Nd, Sr and O in garnet. *Earth and Planetary Science Letters*, **133**, 199–211.

CARSWELL, D. A., WILSON, R. N. & ZHAI, M.-G. 2000. Metamorphic evolution, mineral chemistry and thermobarometry of schists and orthogneisses hosting ultra-high pressure eclogites in the Dabieshan of central China. *Lithos*, **52**, 121–155.

CHACKO, T., XU, X.-S., MAYEDA, T. K., CLAYTON, R. N. & GOLDSMITH, J. R. 1996. Oxygen isotope fractionation in muscovite, phlogopite, and rutile. *Geochimica et Cosmochimica Acta*, **60**, 2595–2608.

CHACKO, T., COLE, D. R. & HORITA, J. 2001. Equilibrium oxygen, hydrogen and carbon isotope fractionation factors applicable to geologic systems. *Reviews in Mineralogy and Geochemistry*, **43**, 1–81.

CHAKRABORTY, S. & GANGULY, J. 1992. Cation diffusion in aluminosilicate garnets: experimental determination in spessartine-almandine diffusion couples, evaluation of effective binary diffusion coefficients, and applications. *Contributions to Mineralogy and Petrology*, **111**, 74–86.

CHAVAGNAC, V., JAHN, B.-M., VILLA, I. M., WHITEHOUSE, M. J. and LIU, D.-Y. 2001. Multi-chronometric evidence for an in situ origin of the ultrahigh-pressure metamorphic terrane of Dabieshan, China. *Journal of Geology*, **109**, 633–646.

CHERNIAK, D. J. 1995. Sr and Nd diffusion in titanite. *Chemical Geology*, **125**, 219–232.

CHERNIAK, D. J. 1996. Strontium diffusion in sanidine and albite, and general comments on strontium diffusion in alkali feldspars. *Geochimica et Cosmochimica Acta*, **60**, 5037–5043.

CHERNIAK, D. J. 1997. An experimental study of strontium and lead diffusion in calcite, and implications for carbonate diagenesis and metamorphism. *Geochimica et Cosmochimica Acta*, **61**, 4173–4179.

CHERNIAK, D. J. 1998. REE diffusion in calcite. *Earth and Planetary Science Letters*, **160**, 273–287.

CHERNIAK, D. J. 2000. Rare earth element diffusion in apatite. *Geochimica et Cosmochimica Acta*, **64**, 3871–3885.

CHERNIAK, D. J. 2003. REE diffusion in feldspar. *Chemical Geology*, **193**, 25–41.

CHERNIAK, D. J. & RYERSON, F. J. 1993. A study of strontium diffusion in apatite using Rutherford backscattering and ion implantation. *Geochimica et Cosmochimica Acta*, **57**, 4653–4662.

CHERNIAK, D. J. & WATSON, E. B. 1992. A study of strontium diffusion in K-feldspar, Na-K feldspar and anorthite using Rutherford Backscattering Spectroscopy. *Earth and Planetary Science Letters*, **113**, 411–425.

CHERNIAK, D. J., HANCHAR, J. M. & WATSON, E. B. 1997. Rare-earth diffusion in zircon. *Chemical Geology*, **134**, 289–301.

CHIBA, H., CHACKO, T., CLAYTON, R. N. & GOLDSMITH, J. R. 1989. Oxygen isotope fractionations involving diopside, forsterite, magnetite, and calcite: Application to geothermometry. *Geochimica et Cosmochimica Acta*, **53**, 2985–2995.

CLAYTON, R. N., GOLDSMITH, J. R. & MAYEDA, T. K. 1989. Oxygen isotope fractionation in quartz, albite, anorthite and calcite. *Geochimica et Cosmochimica Acta*, **53**, 725–733.

CLIFF, R. A. 1985. Isotopic dating in metamorphic belts. *Journal of the Geological Society, London*, **142**, 97–110.

COGHLAN, R. A. N. 1990. *Studies of diffusion transport: grain boundary transport of oxygen in feldspars, diffusion of oxygen, strontium, and REEs in garnet, and thermal histories of granitic intrusions in South-Central Maine using oxygen isotopes.* PhD thesis, Brown University, Providence, USA.

COLE, D. R. & CHAKRABORTY, S. 2001. Rates and mechanisms of isotopic exchange. *Reviews in Mineralogy and Geochemistry*, **43**, 83–223.

CONG, B.-L. 1996. *Ultrahigh-Pressure Metamorphic Rocks in the Dabieshan–Sulu Region of China.* Science Press, Beijing.

CONG, B.-L., ZHAI, M.-G., CARSWELL, D. A., WILSON, R. N., WANG, Q.-C., ZHAO, Z.-Y. & WINDLEY, B. F. 1995. Petrogenesis of ultrahigh-pressure rocks and their country rocks at Shuanghe in the Dabie Mountains, Central China. *European Journal of Mineralogy*, **7**, 119–138.

DODSON, M. H. 1973. Closure temperature in cooling geochronological and petrological systems. *Contributions to Mineralogy and Petrology*, **40**, 259–274.

DODSON, M. H. 1979. Theory of cooling ages. *In:* JAEGER, E. & HUNZIKER, J. C. (eds) *Lecture in Isotope Geology.* Springer-Verlag, Berlin, 194–202.

EILER, J. M., VALLEY, J. W. & BAUMGARTNER, L. P. 1993. A new look at stable isotope thermometry. *Geochimica et Cosmochimica Acta*, **57**, 2571–2583.

EILER, J. M., FARLEY, K. A., VALLEY, J. W., STOLPER, E. M., HAURI, E. & CRAIG, H., 1995. Oxygen isotope evidence against bulk recycled sediment in the source of Pitcairn island lavas. *Nature*, **377**, 138–141.

ELPHICK, S. C., GRAHAM, C. M. & DENNIS, P. F. 1988. An ion probe study of anhydrous oxygen diffusion in anorthite: A comparison with hydrothermal data and some geological implications. *Contributions to Mineralogy and Petrology*, **100**, 490–495.

FARVER, J. R. 1989. Oxygen self-diffusion in diopside with application to cooling rate determinations. *Earth and Planetary Science Letters*, **92**, 386–396.

FARVER, J. R. 1994. Oxygen self-diffusion in calcite: Dependence on temperature and water fugacity. *Earth and Planetary Science Letters*, **121**, 575–587.

FARVER, J. R. & GILETTI, B. J. 1985. Oxygen diffusion in amphiboles. *Geochimica et Cosmochimica Acta*, **49**, 1403–1411.

FARVER, J. R. & GILETTI, B. J. 1989. Oxygen and strontium diffusion kinetics in apatite and their application to cooling rate determination. *Geochimica et Cosmochimica Acta*, **53**, 1621–1631.

FOLAND, K. A. 1974. ^{40}Ar diffusion in homogeneous orthoclase and an interpretation of Ar diffusion in K-feldspars. *Geochimica et Cosmochimica Acta*, **38**, 151–166.

FORTIER, S. M. & GILETTI, B. J. 1991. Volume self-diffusion of oxygen in biotite, muscovite, and phlogopite micas. *Geochimica et Cosmochimica Acta*, **55**, 1319–1330.

FREER, D. J. & EDWARDS, A. 1999. An experimental study of Ca-(Fe, Mg) interdiffusion in silicate garnets. *Contributions to Mineralogy and Petrology*, **134**, 370–379.

FU, B., ZHENG, Y.-F., WANG, Z.-R., XIAO, Y.-L., GONG, B. & LI, S.-G. 1999. Oxygen and hydrogen isotope geochemistry of gneisses associated with ultrahigh pressure eclogites at Shuanghe in the Dabie Mountains. *Contributions to Mineralogy and Petrology*, **134**, 52–66.

GANGULY, J. & RUIZ, J. 1987. Time-temperature relation of mineral isochrons: a thermodynamic model, and illustrative example for the Rb–Sr system. *Earth and Planetary Science Letters*, **81**, 338–348.

GANGULY, J., TIRONE, M. & HERVIG, R. L. 1998. Diffusional kinetics of samarium and neodymium in garnet, and a model for determining cooling rates of rocks. *Science*, **281**, 805–807.

GAUTASON, B., CHACKO, T. & MUEHLENBACHS, K. 1993. Oxygen isotope partitioning among perovskite ($CaTiO_3$), cassiterite (SnO_2) and calcite ($CaCO_3$). *Abstract Program, Joint Meeting GAC and MAC*, Edmonton, A34.

GEBAUER, D. 1990. Isotopic systems – geochronology of eclogites. *In*: CARSWELL, D. A. (ed.) *Eclogite Facies Rocks*. Blackie, Glasgow, 141–159.

GILETTI, B. J. 1974. Studies in diffusion I: Ar in phlogopite mica. *In:* HOFMANN, A. W. *et al.* (eds) *Geochemical Transport and Kinetics.* Carnegie Institute Publication, **634**, 107–115.

GILETTI, B. J. 1985. The nature of oxygen transport within minerals in the presence of hydrothermal water and the role of diffusion. *Chemical Geology*, **53**, 197–206.

GILETTI, B. J. 1986. Diffusion effects on oxygen isotope temperatures of slowly cooled igneous and metamorphic rocks. *Earth and Planetary Science Letters*, **77**, 218–228.

GILETTI, B. J. 1991. Rb and Sr diffusion in alkali feldspars, with implications for cooling histories of rocks. *Geochimica et Cosmochimica Acta*, **55**, 1331–1343.

GILETTI, B. J. 1994. Isotopic equilibrium/disequilibrium and diffusion kinetics in feldspars. *In:* PARSON, I. (ed.) *Feldspars and Their Reactions.* NATO ASI Series C, **421**, 351–382.

GILETTI, B. J. & CASSERLY, J. E. D. 1994. Sr diffusion kinetics in plagioclase feldspars. *Geochimica et Cosmochimica Acta*, **58**, 3785–3793.

GILETTI, B. J. & HESS, K. C. 1988. Oxygen diffusion in magnetite. *Earth and Planetary Science Letters*, **89**, 115–122.

GILETTI, B. J. & YUND, R. A. 1984. Oxygen diffusion in quartz. *Journal of Geophysical Research*, **B89**, 4039–4046.

GILETTI, B. J., SEMET, M. P. & YUND, R. A. 1978. Studies in diffusion, III. Oxygen in feldspars, an ion microprobe determination. *Geochimica et Cosmochimica Acta*, **42**, 45–57.

HAMMOUDA, T. & CHERNIAK, D. J. 2000. Diffusion of Sr in fluorphlogopite by Rutherford Backscattered spectrometry. *Earth and Planetary Science Letters*, **178**, 339–349.

HARRISON, T. M. 1981. Diffusion of ^{40}Ar in hornblende. *Contributions to Mineralogy and Petrology*, **78**, 324–331.

HARRISON, T. M., DUNCAN, I. & MCDOUGALL, I. 1985. Diffusion of ^{40}Ar in biotite: Temperature, pressure and compositional effects. *Geochimica et Cosmochimica Acta*, **49**, 2461–2468.

HOEFS, J. 1997. *Stable Isotope Geochemistry*, 4th edition, Springer-Verlag, Berlin.

JAGOUTZ, E. 1988. Nd and Sr systematics in an eclogite xenolith from Tanzania: Evidence for frozen mineral equilibria in continental lithosphere. *Geochimica et Cosmochimica Acta*, **52**, 1285–1293.

JAVOY, M., FOURCADE, S. & ALLEGRE, C. J. 1970. Graphical method for examination of $^{18}O/^{16}O$ fractionations in silicate rocks. *Earth and Planetary Science Letters*, **10**, 12–16.

JENKIN, G. R. T. 1997. Do cooling paths derived from mica Rb–Sr data reflect true cooling paths? *Geology*, **25**, 907–910.

JENKIN, G. R. T., FARROW, C. M., FALLICK, A. E. & HIGGINS, D. 1994. Oxygen isotope exchange and closure temperatures in cooling rocks. *Journal of Metamorphic Geology*, **12**, 221–235.

JENKIN, G. R. T., ELLAM, R. M., ROGERS, G. & STUART, F. M. 2001. An investigation of closure temperature of the biotite Rb–Sr system: The importance of cation exchange. *Geochimica et Cosmochimica Acta*, **65**, 1141–1160.

LABOTKA, T. C., COLE, D. R. & RICIPUTI, L. R. 2000. Diffusion of C and O in calcite at 100 MPa. *American Mineralogist*, **85**, 488–494.

LI, S.-G., XIAO, Y.-L. *et al.* 1993. Collision of the North China and Yangtse Blocks and formation of coesite-bearing eclogites: Timing and processes. *Chemical Geology*, **109**, 89–111.

LI, S.-G., WANG, S.-S., CHEN, Y.-Z., LIU, D.-L., QIU, J., ZHOU, H.-X. & ZHANG, Z.-M. 1994. Excess argon in phengite from eclogite: Evidence from dating of eclogite minerals by Sm–Nd, Rb–Sr and $^{40}Ar/^{39}Ar$ methods. *Chemical Geology*, **112**, 343–350.

LI, S.-G., LI, H.-M., CHEN, Y.-Z., XIAO, Y.-L. & LIU, D.-L. 1997. Chronology of ultrahigh-pressure metamorphism in the Dabie Mountains and Su–Lu terrane: II. U–Pb isotope system of zircons. *Science China* (D), **40**, 200–206 (in Chinese).

LI, S.-G., JAGOUTZ, E., LO, C.-H., CHEN, Y.-Z., LI, Q.-L. & XIAO, Y.-L. 1999. Sm–Nd, Rb–Sr and $^{40}Ar/^{39}Ar$ isotopic systematics of the ultrahigh pressure metamorphic rocks in the Dabie–Sulu belt, central China: A retrospective view. *International Geology Review*, **41**, 1114–1124.

LI, S.-G., JAGOUTZ, E., CHEN, Y.-Z. & LI, Q.-L. 2000. Sm–Nd and Rb–Sr isotopic chronology and cooling history of ultrahigh pressure metamorphic rocks and their country rocks at Shuanghe in the Dabie Mountains, Central China. *Geochimica et Cosmochimica Acta*, **64**, 1077–1093.

LIOU, J. G., ZHANG, R.-Y., EIDE, E. A., WANG, X. M., ERNST, W. G. & MARUYAMA, S. 1996. Metamorphism and tectonics of high-pressure and ultrahigh-pressure belts in the Dabie-Sulu region, China. *In:* HARRISON, M. T. & YIN, A. (eds) *The Tectonics of Asia.* Cambridge University Press, 300–344.

LIOU, J. G., ZHANG, R.-Y. & JAHN, B.-M. 1997. Petrology, geochemistry and isotope data on a ultrahigh-pressure jadeite quartzite from Shuanghe, Dabie Mountains, East-central China. *Lithos*, **41**, 59–78.

LIU, J. B., YE, K., MARUYAMA, S., CONG, B. L. & FAN, H. R. 2001. Mineral inclusions in zircon from gneisses in the ultrahigh-pressure zone of the Dabie Mountains, China. *Journal of Geology*, **109**, 523–535.

LUAIS, B., DUCHENE, S. & DE SIGOYER, J. 2001. Sm–Nd disequilibrium in high-pressure, low-temperature Himalayan and Alpine rocks. *Tectonophysics*, **342**, 1–22.

MATTHEWS, A., PALIN, J. M., EPSTEIN, S. & STOLPER, E. M. 1994. Experimental study of $^{18}O/^{16}O$ partitioning between crystalline albite, albitic glass, and CO_2 gas. *Geochimica et Cosmochimica Acta*, **58**, 5255–5266.

MORISHITA, Y., GILETTI, B. J. & FARVER, J. R. 1990. Strontium and oxygen self-diffusion in titanite. *Eos*, **71**, 652 (abstract).

MORISHITA, Y., GILETTI, B. J. & FARVER, J. R. 1996. Volume self-diffusion of oxygen in titanite. *Geochemical Journal*, **30**, 71–79.

MORK, M. B. E. & MEARNS, E. W. 1986. Sm–Nd isotopic systematic of the gabbro-eclogite transition. *Lithos*, **19**, 255–267.

MOORE, D. K., CHERNIAK, D. J. & WATSON, E. B. 1998. Oxygen diffusion in rutile from 750 to 1000 °C and 0.1 to 1000 MPa. *American Mineralogist*, **83**, 700–711.

OKAY, A. I. 1993. Petrology of a diamond and coesite-bearing metamorphic terrain: Dabie Shan, China. *European Journal of Mineralogy*, **5**, 659–673.

OKAY, A. I., XU, S.-T. & SENGOR, A. M. C. 1989. Coesite from the Dabie Shan eclogites, central China. *European Journal of Mineralogy*, **1**, 595–598.

POLYAKOV, V. B. & MINEEV, S. D. 2000. The use of Moessbauer spectroscopic data in stable isotope geochemistry. *Geochimica et Cosmochimica Acta*, **64**, 849–865.

ROSENBAUM, J. M. & MATTEY, D. 1995. Equilibrium garnet–calcite oxygen isotope fractionation. *Geochimica et Cosmochimica Acta*, **59**, 2839–2842.

RUMBLE, D., FARQUHAR, J., YOUNG, E. D. & CHRISTENSEN, C. P. 1997. In situ oxygen isotope analysis with an excimer laser using F_2 and BrF_5 reagents and O_2 gas as analyte. *Geochimica et Cosmochimica Acta*, **61**, 4229–4234.

SCHMAEDICKE, E., MEZGER, K., COSCA, M. A. & OKRUSCH, M. 1995. Variscan Sm–Nd and Ar–Ar ages of eclogite facies rocks from the Erzgebirg, Bohemian Massif. *Journal of Metamorphic Geology*, **13**, 537–552.

SHARP, Z. D. 1990. A laser-based microanalytical method for the in situ determination of oxygen isotope ratios of silicates and oxides. *Geochimica et Cosmochimica Acta*, **54**, 1353–1357.

SHARP, Z. D. 1995. Oxygen isotope geochemistry of the Al_2SiO_5 polymorphs. *American Journal of Science*, **295**, 1058–1076.

SHARP, Z. D. & KIRSCHNER, D. L. 1994. Quartz–calcite oxygen isotope thermometry: A calibration based on natural isotopic variations. *Geochimica et Cosmochimica Acta*, **58**, 4491–4501.

SHARP, Z. D., GILETTI, B. J. & YODER, H. S. Jr. 1991. Oxygen diffusion rates in quartz exchanged with CO_2. *Earth and Planetary Science Letters*, **107**, 339–348.

SNEERINGER, M., HART, S. R. & SHIMIZU, N. 1984. Strontium and samarium diffusion in diopside. *Geochimica et Cosmochimica Acta*, **48**, 1589–1608.

STOWELL, H. H. & GOLDBERG, S. A. 1997. Sm–Nd garnet dating of polyphase metamorphism: northern Coast Mountains, south-eastern Alaska, USA. *Journal of Metamorphic Geology*, **15**, 439–450.

TENNIE, A., HOFFBAUER, R. & HOERNES, S. 1998. The oxygen isotope fractionation behavior of kyanite in experiment and nature. *Contributions to Mineralogy and Petrology*, **133**, 346–355.

THOENI, M. 2002. Sm–Nd isotope systematics in garnet from different lithologies (Eastern Alps): age results, and an evaluation of potential problems for garnet Sm-Nd chronometry. *Chemical Geology*, **185**, 255–281.

THOENI, M. & JAGOUTZ, E. 1992. Some new aspects of dating eclogites in orogenic belts: Sm–Nd, Rb–Sr and Pb–Pb isotopic results from the Austroalpine Saualpe and Koralpe type-locality. *Geochimica et Cosmochimica Acta*, **56**, 347–368.

VALLEY, J. W. 2001. Stable isotope thermometry at high temperatures. *Reviews in Mineralogy and Geochemistry*, **43**, 365–413.

VALLEY, J. W., KITCHEN, N., KOHN, M. J., NIENDORF, C. R. & SPICUZZA, M. J. 1995. UWG-2, a garnet standard for oxygen isotope ratio: strategies for high precision and accuracy with laser heating. *Geochimica et Cosmochimica Acta*, **59**, 5223–5231.

VANCE, D. & HARRIS, N. 1999. Timing of prograde metamorphism in the Zabskar Himalaya. Geology, **27**, 395–398.

VANCE, D. & HOLLAND, T. 1993. A detailed isotopic and petrological study of a single garnet from the Gassetts Schist, Vermont. *Contributions to Mineralogy and Petrology*, **114**, 101–118.

VANCE, D. & O'NIONS, R. K. 1990. Isotopic chronometry of zoned garnets: growth kinetics and metamorphic histories. *Earth and Planetary Science Letters*, **97**, 227–240.

VANCE, D. & O'NIONS, R. K. 1992. Prograde and retrograde thermal histories from the central Swiss Alps. *Earth and Planetary Science Letters*, **114**, 113–129.

VAN ORMAN, J. A., GROVE, T. L. & SHIMIZU, N. 2001. Rare earth element diffusion in diopside: influence of temperature, pressure, and ionic radius, and an elastic model for diffusion in silicates. *Contributions to Mineralogy and Petrology*, **141**, 687–703.

VAN ORMAN, J. A., GROVE, T. L., SHIMIZU, N. & LAYNE, G. D. 2002. Rare earth element diffusion in a natural pyrope single crystal at 2.8 GPa. *Contributions to Mineralogy and Petrology*, **142**, 416–424.

WANG, X.-M., LIOU, J. G. and MAO, H.-K. 1989. Coesites-bearing from the Dabie Mountains in central China. *Geology*, **17**, 1085–1088.

WANG, X. M., ZHANG, R. Y. & LIOU, J. G. 1995. UHPM terrane in east central China. *In:* COLEMAN, R. & WANG, X. (eds) *Ultrahigh Pressure Metamorphism.* Cambridge University Press, 356–390.

WATSON, E. B. & CHERNIAK, D. J. 1997. Oxygen diffusion in zircon. *Earth and Planetary Science Letters*, **148**, 527–544.

WATSON, E. B., HARRISON, T. M. & RYERSON, F. J. 1985. Diffusion of Sm, Ar and Pb in fluorapatite. *Geochimica et Cosmochimica Acta*, **49**, 1813–1823.

XIAO, Y.-L., HOEFS, J., VAN DEN KERKHOF, A. M., FIEBIG, J. & ZHENG, Y.-F. 2000. Fluid history of UHP metamorphism in Dabie Shan, China: a fluid inclusion and oxygen isotope study on the coesite-bearing eclogite from Bixiling. *Contributions to Mineralogy and Petrology*, **139**, 1–16.

XIAO, Y.-L., HOEFS, J., VAN DEN KERKHOF, A. M., SIMON, K., FIEBIG, J. & ZHENG, Y.-F. 2002. Fluid evolution during HP and UHP metamorphism in Dabie Shan, China: Constraints from mineral chemistry, fluid inclusions and stable isotopes. *Journal of Petrology*, **43**, 1505–1527.

XU, B.-L. & ZHENG, Y.-F. 1999. Experimental studies of oxygen and hydrogen isotope fractionations between precipitated brucite and water at low temperatures. *Geochimica et Cosmochimica Acta*, **63**, 2009–2018.

XU, S.-T., OKAY, A. I., JI, S.-Y., SENGOR, A. M. C., SU, W., LIU, Y.-C. & JIANG, L.-L. 1992. Diamond from the Dabie Shan metamorphic rocks and its

implication for tectonic setting. *Science*, **256**, 80–82.

YUI, T.-F., RUMBLE, III D., CHEN, C.-H. & LO, C.-H. 1997. Stable isotope characteristics of eclogites from the ultra-high-pressure metamorphic terrain, east-central China. *Chemical Geology*, **137**, 135–147.

ZHANG, L.-G., LIU, J.-X., CHEN, Z.-S. & ZHOU, H.-B. 1994. Experimental investigations of oxygen isotope fractionation in cassiterite and wolframite. *Economic Geology*, **89**, 150–157.

ZHANG, R. Y., LIOU, J. G., ZHENG, Y.-F. & FU, B. 2003. Transition of UHP eclogites to gneissic rocks of low-grade amphibolite facies during exhumation: Evidence from the Dabie terrane, central China. *Lithos*, **70**, 101–125.

ZHENG, Y.-F. 1989. Influence of the nature of the initial Rb–Sr system on isochron validity. *Chemical Geology*, **80**, 1–16.

ZHENG, Y.-F. 1990. A further three-dimensional U–Pb method for solving the two-stage episodic model. *Geochemical Journal*, **24**, 29–37.

ZHENG, Y.-F. 1991. Calculation of oxygen isotope fractionation in metal oxides. *Geochimica et Cosmochimica Acta*, **55**, 2299–2307.

ZHENG, Y.-F. 1992*a*. Oxygen isotope fractionation in wolframite. European *Journal of Mineralogy*, **4**, 1331–1335.

ZHENG, Y.-F. 1992*b*. The three-dimensional U–Pb method: Generalized models and implications for U–Pb two-stage systematics. Chemical Geology, **100**, 3–18.

ZHENG, Y.-F. 1993*a*. Calculation of oxygen isotope fractionation in anhydrous silicate minerals. *Geochimica et Cosmochimica Acta*, **57**, 1079–1091.

ZHENG, Y.-F. 1993*b*. Calculation of oxygen isotope fractionation in hydroxyl-bearing minerals. *Earth and Planetary Science Letters*, **120**, 247–263.

ZHENG, Y.-F. 1993*c*. Oxygen isotope fractionation in SiO_2 and Al_2SiO_5 polymorphs: effect of crystal structure. European *Journal of Mineralogy*, **5**, 651–658.

ZHENG, Y.-F. 1995. Oxygen isotope fractionation in magnetites: structural effect and oxygen inheritance. *Chemical Geology*, **121**, 309–316.

ZHENG, Y.-F. 1996*a*. Oxygen isotope fractionations involving apatites: Application to paleotemperature determination. *Chemical Geology*, **127**, 177–187.

ZHENG, Y.-F. 1996*b*. Oxygen isotope fractionation in zinc oxides and implications for zinc mineralization in the Sterling Hill deposit, USA. *Mineralium Deposita*, **31**, 98–103.

ZHENG, Y.-F. 1997. Prediction of high-temperature oxygen isotope fractionation factors between mantle minerals. *Physics and Chemistry of Minerals*, **24**, 356–364.

ZHENG, Y.-F. 1998. Oxygen isotope fractionation between hydroxide minerals and water. *Physics and Chemistry of Minerals*, **25**, 213–221.

ZHENG, Y.-F. 1999*a*. Oxygen isotope fractionation in carbonate and sulfate minerals. *Geochemical Journal*, **33**, 109–126.

ZHENG, Y.-F. 1999*b*. On calculations of oxygen isotope fractionation in minerals. *Episodes*, **22**, 99–106.

ZHENG, Y.-F. & FU, B. 1998. Estimation of oxygen diffusivity from anion porosity in minerals. *Geochemical Journal*, **32**, 71–89.

ZHENG, Y.-F., METZ, P. & SATIR, M. 1994. Oxygen isotope fractionation between calcite and tremolite: an experimental study. *Contributions to Mineralogy and Petrology*, **118**, 249–255.

ZHENG, Y.-F., FU, B., GONG, B. & LI, S.-G. 1996. Extreme ^{18}O depletion in eclogite from the Su–Lu terrane in East China. *European Journal of Mineralogy*, **8**, 317–323.

ZHENG, Y.-F., FU, B., LI, Y.-L., XIAO, Y.-L. & LI, S.-G. 1998. Oxygen and hydrogen isotope geochemistry of ultrahigh pressure eclogites from the Dabie Mountains and the Sulu terrane. *Earth and Planetary Science Letters*, **155**, 113–129.

ZHENG, Y.-F., FU, B., XIAO, Y.-L., LI, Y.-L. & GONG, B. 1999. Hydrogen and oxygen isotope evidence for fluid-rock interactions in the stages of pre- and post-UHP metamorphism in the Dabie Mountains. *Lithos*, **46**, 677–693.

ZHENG, Y.-F., GONG, B., LI, Y.-L., WANG, Z.-R. & FU, B. 2000. Carbon concentrations and isotopic ratios of eclogites from the Dabie and Sulu terranes in China. *Chemical Geology*, **168**, 291–305.

ZHENG, Y.-F., FU, B., LI, Y.-L., WEI, C.-S. & ZHOU, J.-B. 2001. Oxygen isotope composition of granulites from Dabieshan in eastern China and its implications for geodynamics of Yangtze plate subduction. *Physical Chemistry of the Earth* (A), **26**, 673–684.

ZHENG, Y.-F., WANG, Z.-R., LI, S.-G. & ZHAO, Z.-F. 2002. Oxygen isotope equilibrium between eclogite minerals and its constraints on mineral Sm–Nd chronometer. *Geochimica et Cosmochimica Acta*, **66**, 625–634.

ZHENG, Y.-F., GONG, B., ZHAO, Z.-F., FU, B. & LI, Y.-L. 2003. Two types of gneisses associated with eclogite at Shuanghe in the Dabie terrane: carbon isotope, zircon U–Pb dating and oxygen isotope. *Lithos*, **70**, 161–185.

ZHOU, G.-T. & ZHENG, Y.-F. 2002. Kinetic mechanism of oxygen isotope disequilibrium in precipitated witherite and aragonite at low temperatures: An experimental study. *Geochimica et Cosmochimica Acta*, **66**, 63–71.

ZHOU, G.-T. & ZHENG, Y.-F. 2003. An experimental study of oxygen isotope fractionation between inorganically precipitated aragonite and water at low temperatures. *Geochimica et Cosmochimica Acta*, **67**, 387–399.